Journal of Sedimentary Environments
https://doi.org/10.1007/s43217-022-00103-9

ORIGINAL ARTICLE

Long-time impact of a large dam on its downstream river's morphology: determined by sediment characteristics, pollutants as a marker, and numerical modelling

Stefanie Wolf[1] · Verena Esser[2] · Frank Lehmkuhl[2] · Holger Schüttrumpf[1]

Received: 7 March 2022 / Revised: 27 April 2022 / Accepted: 1 May 2022

Abstract
Many river systems are regulated by dams, which causes an altered flow regime and sediment deficit in the downstream reach. The Rur dam (North Rhine-Westphalia, Germany), constructed from 1900 to 1959, serves as a model example of the impact of a large dam in a European low mountain area on downstream morphology. Today, a new equilibrium incorporates flow regulations, a deficit in suspended sediment supply, and an increased mean sediment diameter downstream of the dam. A hybrid examination of field measurements and numerical modelling shows that the sediment deficit and increased mean sediment diameters downstream of the Rur dam are superimposed by the lithostratigraphy and the sediment supply of tributaries. However, the discharge regulations lead to floodplain decoupling downstream of the dam. Furthermore, the Rur dam functions as a pollutant trap. Overall, more studies on the impact of damming on downstream reaches are needed to classify the impact depending on the river type for sustainable water management.

Keywords Long-time impact of large dam · Downstream morphodynamics · Dams in context of pollutants · Floodplain decoupling

1 Background

Today, 60% of the world's rivers' runoff is affected by dams (Nilsson et al., 2005). Since the mid-twentieth century, dam construction has been booming worldwide. In the 1960s and 1970s, the peak of dam construction was reached with about 150 km^3 of new storage from 130 new reservoirs per year (Wisser et al., 2013). By 2010, 40% of the worldwide land surface drain into dams (Wisser et al., 2013). However, most of the reservoirs worldwide are relatively small, since a lot of them have a residence time of water renewal of less than a year (Wisser et al., 2013).

The main reasons for dam construction worldwide are balancing floods and droughts to provide a steady water supply and reduce flood damage (e.g., Beaumont, 1983; Dai & Liu, 2013). In addition, almost two-thirds of all reservoirs also serve to generate electricity from hydropower (Wisser et al., 2013). In the nineteenth century, adjacent industries on the Rur River were affected by yearly flood events as well as dry seasons during the summer (Wasserverband Eifel-Rur, 1999). The increased water demand of local industries led to a water crisis and ultimately to the construction of large dams on the Rur River from 1900 onwards (Lehmkuhl, 2011; Nilson & Lehmkuhl, 2006; Paul, 1994). Hence, the Rur and Urft dams were built for water supply, flood control as well as energy supply (Intze, 1906; Wasserverband Eifel-Rur, 1999).

Reservoirs function as a sedimentation basin, and not only coarser sediment but also parts of the fine fraction are retained (Kondolf, 1995). Wisser et al. (2013) found, that

Communicated by M. V. Alves Martins.

✉ Stefanie Wolf
wolf@iww.rwth-aachen.de

Verena Esser
verena.esser@geo.rwth-aachen.de

Frank Lehmkuhl
flehmkuhl@geo.rwth-aachen.de

Holger Schüttrumpf
schuettrumpf@iww.rwth-aachen.de

[1] Institute for Hydraulic Engineering and Water Resources Management, RWTH Aachen University, Mies-van-der-Rohe-Straße 17, 52056 Aachen, Germany

[2] Department of Geography, RWTH Aachen University, Wüllnerstraße 5b, 52064 Aachen, Germany

Published online: 26 May 2022

worldwide, the mean reservoir loss due to sedimentation is 0.55% of the storage volume per year. Therefore, a lot of studies investigate reservoir sedimentation and storage loss (e.g., Annandale, 2013; Issa et al., 2015; Rahmani et al., 2018; Saam et al., 2019; Wisser et al., 2013; Yang et al., 2007, 2014). In addition, many researchers investigate estuary and coastal erosion caused by sediment deficits downstream of dams (e.g., Dai & Liu, 2013; Kondolf, 1997; Luo et al., 2012; Rovira & Ibàñez, 2007; van Maren et al., 2013; Walling, 2012; Yang et al., 2014). Many studies as well focus on morphologic channel changes due to dam construction (e.g., Adib et al., 2016; Assani & Petit, 2004; Brousse et al., 2020; Dai & Liu, 2013; Dai & Liu, 2013; Grams et al., 2007; Nelson et al., 2013; Petts, 1979; Phillips et al., 2005; Yang et al., 2014), in river systems which are rich in fine materials, or dam removal as well as dam failure (e.g., Major et al. 2012; East et al., 2015; Kibler et al., 2011). Possible impacts on downstreams' morphology are summed up in Table 1. Studies incorporating numerical modelling downstream of large dams mainly focus on case scenarios of dam failure, dam deconstruction, or the impact of sediment flushing or storage loss (e.g., Elsaeed et al., 2018; Gelfenbaum et al., 2015; Mool et al., 2017; Morgan & Nelson, 2019; Saam et al., 2019), but not on long term impacts of large dams. Out of only six fitting results for "large dam(s), "numerical model" or "simulation" and "river" on Web of Science, only one study examines the morphological impact downstream of a large dam (Sanyal et al., 2021). However, this study by Sanyal et al. (2021) examines the Godavari River (India) which is rich in clay and silt and transports large amounts of suspended matter (Biksham & Subramanian, 1988). The other studies cover risk assessments, biodiversity and reservoir management. Concluding, a research gap exists in determining the long-time impact of large dams on downstream reaches, especially in river systems rich in coarse materials.

1.1 Impact of the regulated sediment transport and discharge

Changes the in composition of transported sediments start upstream of the dam following a sedimentation pattern, in which first non-cohesive sediment, such as gravel and sand, gets deposited. Subsequently, sediment composition gets finer closer to the dam (Ziegler & Nisbet, 1995), since finer sediments are deposited due to reduced flow velocities (Ziegler & Nisbet, 1995). The output of a dam to the downstream river can be divided into an altered water flow and a reduced sediment discharge (Brandt, 2000; Schmidt & Wilcock, 2008). Williams and Wolman (1984) detected reduced suspended sediment concentrations (SSCs) downstream of large dams. Consequently, the riverbed coarsens, because fine bed material is eroded downstream of the dam, but is not replaced (Kondolf, 1997). Therefore, an increase in the mean particle diameter often is observed over time (Williams and Wolman 1984; Yang et al., 2014), as in the Glen Canyon, where the mean diameter increased from 0.25 to 20 mm within 43 years after dam construction (Grams et al., 2007). However, impacts can be different for river systems, which are rich in fine materials (e.g., van Maren et al., 2013).

The development of an amour layer comes with coarsening of the riverbed, often caused by a deficit in fine sediments downstream of large dams (e.g., Bunte, 2004). Bed armouring and clustering of particles also occurs when the discharge is constant over a longer period (Sutherland, 1987). Higher discharges are necessary to mobilize sediments when an armour layer has formed (e.g., Kondolf, 1997; Petts, 1979; Rollet et al., 2014; Rovira & Ibàñez, 2007).

Bunte (2004) has observed reductions of high flows down to 10–20% and an increase in baseflow up to 50–100% downstream of large dams. However, channel degradation downstream of dams as a result of general sediment deficits caused by dams is very common (Petts, 1979), but depends on various factors. Hence, Williams and Wolman (1984) detected bed degradations varying from neglectable depths to about 7.5 m. They also detected varying changes in channel width from an increase of 100% to a decrease of 90% (Williams & Wolman, 1984). In any case, in the long run, an equilibrium will form between the flow capacity, released sediments from the reservoir, and the erosivity of the flow together with the erodibility of river banks (Brandt, 2000).

Table 1 Summary of possible impact of damming on downstreams' morphology

Possible impact of damming on downstreams morphology	Due to…	Sources
Coarsening of the riverbed, increase of mean particle diameter	Sediment deficit	Grams et al., (2007), Kondolf (1997), Williams and Wolman (1984) and Yang et al., (2014)
Bed armouring	Sediment deficit, discharge regulation	Bunte (2004) and Sutherland (1987)
Bed narrowing	Reduction of flood events	Kondolf (1997)
Bed degradation	Sediment deficit	Petts (1979) and Williams and Wolman (1984)
Pollutant reduction	Sediment trapping	Palanques et al., (2014) and Ziegler and Nisbet (1995)

1.2 Dams in the context of pollutants

Trace elements such as Cu and Pb occur naturally in soils and rocks, depending on the geological setting. The concentrations vary highly, depending on the region (Fauth, 1985). Anthropogenic sources such as mining, industries, traffic, settlements, or agriculture cause enrichments and subsequent distribution in the environment (Clark et al., 2014; Anderson, 1996; Callender, 2005; Hillenbrand et al., 2005; Legret & Pagotto, 1999; MKULNV NRW, 2015; Monaci & Bargagli, 1997; UMWELTBUNDESAMT, 2001; Meybeck et al., 2007).

In certain concentrations, different trace elements are necessary for organisms (Kabata-Pendias, 2011); higher concentrations can be toxic and pollute the environment (Foulds et al., 2014; MacDonald et al., 2000). The distribution of trace elements or pollutants, which are especially bound to the fine sediment fraction, is connected to sediment transport in river catchments (Cofalla, 2015; Salomons & Förstner, 1984). Their concentration depends on the location and the type of sources (Walling et al., 2003). Due to natural fluvial processes, the contaminants can be transported over long distances (Miller et al., 1999) as well as stored in the riverbed, floodplains, or in paleo channels for long time (Dhivert et al., 2015; Walling et al., 2003). Hence, contamination can be traced back to historical periods, such as industrialization, which was characterized by strong environmental pollution (Resongles et al., 2014). Through remobilization during flood events, contaminated sediments can enter again into the fluvial system (Ciszewski & Grygar, 2016; Hollert et al., 2014). Nevertheless, the re-input of contaminated sediments can be reduced by water engineering measures, such as channelization (Ciszewski & Grygar, 2016). As discussed before, dam construction does not only modify the natural water discharge of a river, it influences the sediment flux as well. Sediments and sediment-bound trace elements can be stored within the reservoir (Palanques et al., 2014; Ziegler & Nisbet, 1995). Thus, sediment samples taken in reservoirs represent catchment representative trace element concentrations, consisting of natural and anthropogenic signals (Frémion et al., 2016; Palanques et al., 2014; Sojka et al., 2019; Szarek-Gwiazda et al., 2011; Zhao et al., 2013).

On one side, the storing of sediments connected with a reduction of trace elements can improve environmental issues downstream (Bi et al., 2014). On the other side, the reduction of essentials trace elements can have negative effects on creatures, such as copepods (Turner et al., 1998). Nevertheless, in times of sediment release from dams, sediment flux can be characterized by high enrichments of pollutants (Bi et al., 2014). In case of environmental and human health issues downstream, the removal of contaminated dam sediments can be necessary (Palanques et al., 2014).

1.3 Scope of the study

Different research studies show that sediment deficits predominate downstream of dams (e.g., Williams & Wolman, 1984; Brousse et al., 2020, Dai & Liu, 2013; Schmidt & Wilcock, 2008). In addition, an increase in the grain size diameter is observed in rivers rich in coarse materials (e.g., Williams & Wolman, 1984; Kondolf, 1997). Last, dams alter the flow regime, often reducing the mean annual discharge (e.g., Chen et al., 2001; Ibàñez et al., 1996). Hence, the main influences of dams are *sediment deficit* and *reduced* mean annual *discharge* combined with reduced peak flows. The *sediment deficit* can lead to higher riverbed erosion and channel degradation, whereas the *reduced discharge* can lead to channel narrowing. Linked effects to the *sediment deficit* are riverbed erosion, bed armouring, and an increased mean particle diameter. Changes in the amount and characteristics of sediment flux have impacts on the dispersion of sediment-bound pollutants. In our study, we aim to evaluate the three main impacts of the Rur dam, (1) sediment deficit, (2) flow alteration, and (3) increase in grain size diameter, on the downstream morphodynamics. Since the causes of river degradation and poor ecological quality are often not obvious, but many rivers are dammed, a greater understanding of processes is needed to improve stream development in the future. Knowledge of the described impact factors should be included in future projects, such as river restoration, even for river types rich in coarse sediments, which's affection by damming is not obvious at first sight, since the retained fine fraction is low.

2 Study area

In this study, we are investigating 54 km out of the 165 km long Rur River in the 2361 km^2 large Rur catchment (North Rhine-Westphalia, Germany). The Rur River is a typical European upland-to-lowland river with its source and upper reach in the mid-mountainous area of the northern Eifel Mountains. The sources are located in the swamp "High Fens" in Belgium at 600 m.a.s.l. The middle and lower reach of the Rur River are located in the lowlands of the Lower Rhine Embayment in Germany. At 30 m.a.s.l., in the Dutch city of Roermond, is its mouth into the Maas River (Nilson, 2006a; Polczyk, 1999a; Wasserverband Eifel-Rur, 1999) (see Fig. 1).

Corresponding to the characteristics of typical mid-mountain rivers, the morphodynamical processes of the Rur River are shaped by highly variable discharges (Polczyk, 1999a). In the past, contradictory scenarios, such as flood

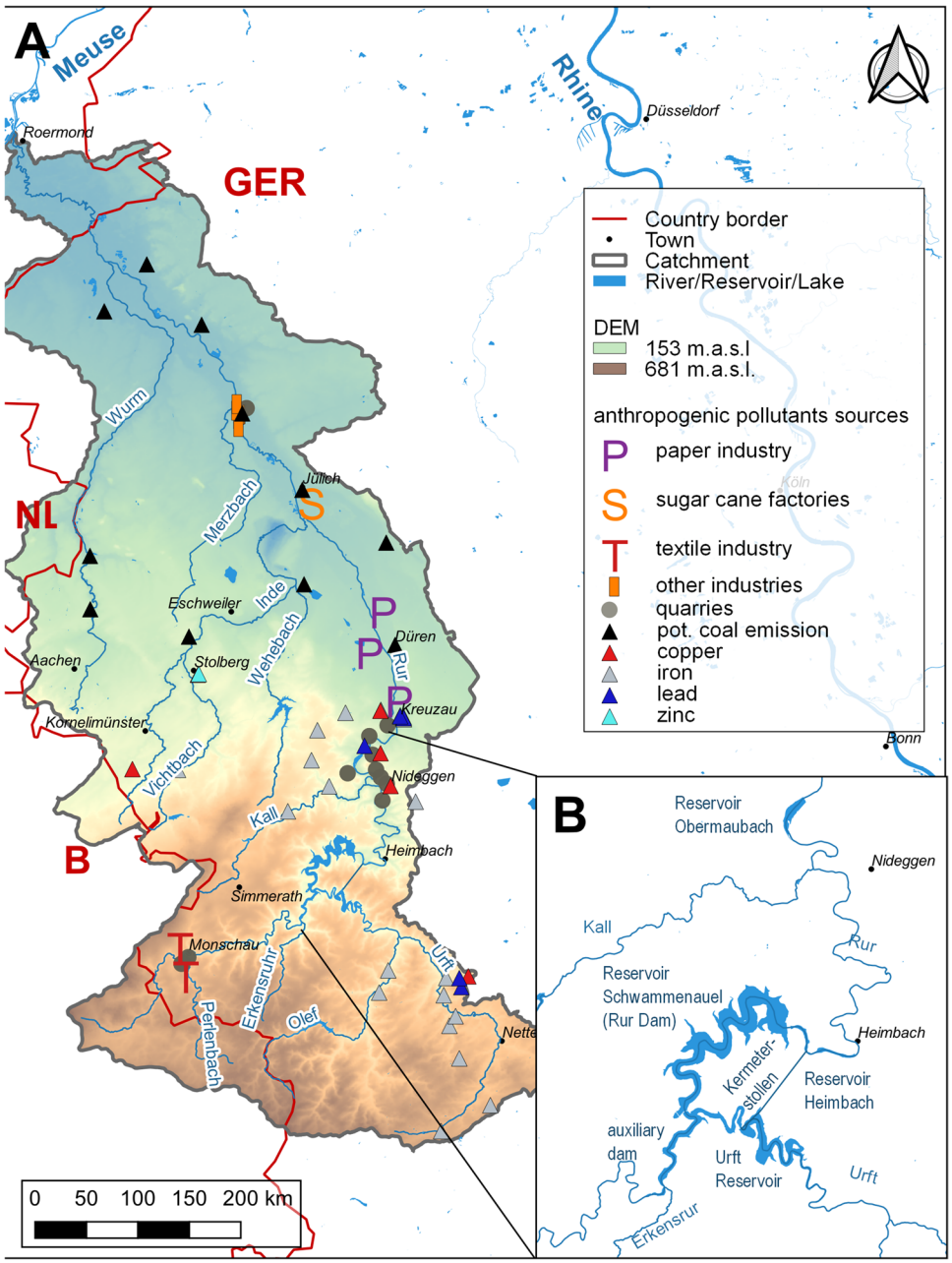

Fig. 1 Overview over the Rur catchment, **A** Rur catchment with potential sources for pollution, **B** source: own illustration; DEM: Bezirksregierung Köln (2021), river system: Geofabrik GmbH (2018), country borders: Eurostat (2020), sources for pollution: Esser (2020) and Wolf et al. (2021)

events or the lack of water caused problems for water-intensive industries, agriculture, and settlements along the Rur River (Paul, 1994). To combat this, large dams on the Urft and Rur River were constructed and hydraulic construction methods were conducted (Polczyk, 1999b). First, the Urft dam was constructed from 1900 to 1905 with a volume of 45.51 hm^3 (Polczyk, 1999a) then the Rur dam, called Rurtalsperre Schwammenauel, was constructed from 1934 to 1938 and upgraded from 1955 to 1959 (Wasserverband Eifel-Rur, 2017a). Together with the Rur dam, the Heimbach reservoir and Obermaubach basin were constructed in 1934/1935 (Wasserverband Eifel-Rur, 2017b, 2017c). Today, the Rurtalsperre Schwammenauel is the main reservoir (Polczyk, 1999a), composed of two dams, dividing the area into an upper lake and the main lake (Wasserverband Eifel-Rur, 2017a). The reservoir has an upstream auxiliary dam (Wasserverband Eifel-Rur, 2017a) and, therefore, no problems with siltation. Two main rivers flow in the reservoir, the Rur River itself and the Urft River. The Rurtalsperre Schwammenauel has a capacity of 203 hm^3 (Wasserverband Eifel-Rur, 2017a). Immediately, this basin is followed by the Heimbach reservoir, which is connected with the Urft reservoir through an adit called "Kermeterstollen" (see Fig. 1). Approx. 18 river km (rkm) after this dam, the last basin in Obermaubach follows (Ministerium für Umwelt, Landwirtschaft, Natur- und Verbraucherschutz NRW 2021).

The area upstream of the Rur dam has a mean annual precipitation of 1000 mm, of which 55 to 60% are relevant for runoff (Polczyk, 1999a). The dams have a total volume of 300 million m^3. 70 million m^3 of the total volume is for flood prevention, 80 million m^3 water per year is used for water supply (Polczyk, 1999a).

Over time, the sediment budget of the Rur River in the upper reach was influenced by diverse land use changes, such as deforestation, reforestation, changes from arable land to grassland, and hydraulic constructions (Nilson, 2006b; Wolf et al., 2021). In the nineteenth century, soil erosion as consequence of deforestation for the high industrial wood-demand caused serious problems for the water management in the study area. Large amounts of bedload are reported (Paul, 1994). During the last 200 years, morphologic indicators show a trend toward more stable sediment dynamics due to human impact (Wolf et al., 2021). Connected with sediment fluxes are sediment-bound pollutants derived from anthropogenic sources, such as mining sites and industry (Esser et al., 2020). In the study area, different industrial sectors were established over time (cf. Figure 1). The city of Monschau was an important centre of textile companies causing water pollution (Paul, 1994; Scheuch, 1967). Various substances were used for textile dyeing, such as "Kupferroth" (mineral Cuprite; Cu_2O). Lead and copper ore mining and its processing were important industries in the sub-catchment of the Urft River (Blass & Graf, 1995; Weiss, 1990a). In the east of the Obermaubach basin, lead- and copper-ore were mined and in the north, lead-ore was extracted (Weiss, 1990a). Between the cities of Kreuzau and Düren a centre of paper industries was established leading to the introduction of wastewater into the river (Scheuch, 1967).

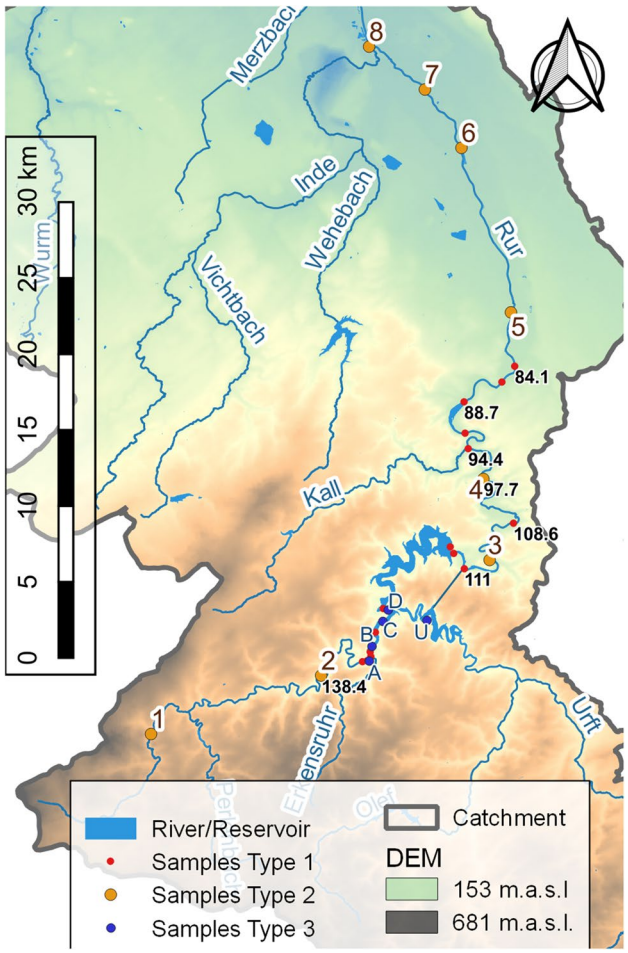

Fig. 2 Sampling points of different samples in this study; red: samples of type 1, investigating the short-time transported sediments, labels show rkm at sampling location, orange: samples of type 2, investigating the sedimentological riverbed composition, labels show the number of sample, blue: samples of riverbed accumulations, **A** to **D** taken in a previous study in the auxiliary dam of the Rur dam, U taken in the Urft reservoir in a currently ongoing study (unpublished)

3 Methods

To evaluate the impact of the mail influences of the Rur dam, *sediment deficit*, *reduced* mean annual *discharge* and *increased mean particle diameter* downstream of the dam, we use different interdisciplinary methods for different subquestions that together yield overarching insights. These can be divided into (1) sedimentary studies and (2) modelling studies:

The suspended sediment transport upstream, within and downstream of the dammed area to determine the sediment deficit in the suspension load (cf. Figure 2). Effects on mean particle diameters and sediment deficits in larger grain size fractions are evaluated from bulk samples of the riverbed and bed of the auxiliary dam of the reservoir Schwammenauel (Fig. 2). In addition, we use heavy metals as markers to evaluate the sediment transport. For that, different sediment samples from the riverbed of the Rur River and dam sediments were analysed. Sediment samples of recent sediments were taken at the same locations at which the suspended sediment concentration in the Rur River was repeatedly measured (cf. Figure 2).

The effect of discharge regulation is examined in a numerical simulation using Delft3D. Furthermore, with the numerical case study, the impact of the dam on downstream erosion and sedimentation can be evaluated, since the model does not cover an overlap with impacts of the lithostratigraphy and slope erosion.

3.1 Sediment studies

The conducted sediment studies include research on different sediment fractions deposits. Three types of samples can be distinguished to evaluate different transport processes and characteristic (cf. Figure 2):

Type 1, short-time transported sediments, includes fine sediments, which are easily mobilized. They are transported in suspension and stored in intermediate storages within the riverbed for a short duration of time. During flood events, these sediment fractions can be deposited on floodplains. Sediments of type 1 give an insight in highly responsive sediment fractions. Type 2 includes sampling and evaluating the sedimentological riverbed composition. For type 2 not the dynamic transport processes, but the current status of the riverbed composition is of interest. Type 3 are samples of dam accumulations. Those samples provide additional information, which helps with the evaluation and interpretation of samples of type 1 and 2.

3.1.1 Type 1: short-time transported sediments

Type 1 samples consist of water samples containing suspended sediments (SSC) and sediment samples from the riverbed embankments. Both samples were sampled in combined field trips from October 16th, 2019 until July 22nd, 2021. Samples were taken at low and high discharge, following an annual discharge pattern. Sampling of sediments from the riverbed embankments was not possible in some areas with bank protection (cf. Supplement A, Tables 1 and 2). Furthermore, an extreme flood event in the mid of July 2021 was sampled. During this flood event, inflows of up to 500 m^3/s into the Rur dam were recorded (Reichert, 2021). According to initial projections, the event is s considered to be a 1000-year flood (Reichert, 2021). Sampling was carried out during the event and after the flood had subsided, but discharge from the dams was still high as dam discharge was increased (Reichert, 2021; Wasserverband Eifel-Rur, 2021). During the flood event, on July 15th, 2021, some sampling sites were not accessible (cf. Supplement A, Table 2).

3.1.2 SSC

For investigating SSC, in total 119 samples of 2×0.5 or 1 L (sample and reference sample) from 17 sampling sites were taken along the Rur River and in the dammed area from October 16th, 2019 until July 15th, 2021 (Supplement A, Table 1 and Fig. 2, please note, that two samples were taken at the spillway at rkm 123.20 and rkm 111.05 during the flood event). This includes samples from a sampling point before the backwater of the Rur dam influences the river's flow and samples from two sampling points downstream of the second reservoir, the Obermaubach basin. On October 11th, 2020 the auxiliary basin of the Rur basin Schwammenauel was fallen dry for maintenance reasons, why we could not access sampling points from rkm 127.70 to rkm 123.20. In addition, the sampling of the dammed section of the Rur River was included in a larger sampling campaign along the Rur River, wherefore more samples exist from river sections up- and downstream of the dammed area (rkm 138.4, rkm 97.70–rkm 84.1).

The sediment concentration of the water samples was determined by filtration using a vacuum pump as described in Maaß and Schüttrumpf (2019b).

3.1.3 Highly mobile riverbed accumulations

In this study, we use the sediment-bound trace elements Pb and Cu. Composite samples of riverbed sediments were taken from the upper first centimetre of the riverbed and flood sediment accumulations were sampled on the floodplains after the flood events in January 2021 and in July 2021. Sampling locations can be found in Supplement A, Table 2.

For XRF-Analysis all sampled were sieved (< 63 µm), the fine fraction < 63 µm was dried at 105 °C for 12 h, and 8 g of sieved material and 2 g wax (Fluxana Cereox) were mixed, homogenized, and pressed to a pellet (pressure of 19.2 MPa for 120 s). All pellets were analysed twice using an energy dispersive polarized Spectro Xepos X-ray fluorescence (XRF) device. Afterwards, mean values were calculated from the two measurements (cf. SPECTRO, 2007 for further information).

3.1.4 Data evaluation

Afterwards, samples are sorted by discharge conditions present during sampling. With data from the nearest gauging station, the values were divided into samples taken at low to mid discharge and samples taken at mid to high discharge (cf. Supplement A, Table 3). Discharges below mean discharge (MQ) are considered low to mid discharge and discharges above MQ are considered mid to high discharges. No values exceeded flood events with a 5-years annularity (HQ5) or were below an average low discharge between October 2019 to February 2021. The recent flood event in July 2021 exceeded all flows in the previous sampling periods and is evaluated separately.

3.1.5 Type 2: Sedimentological riverbed composition

Bulk samples of the riverbed were taken at eight sampling points along the Rur River from the uplands to the lowlands (cf. Figure 2 and Supplement A, Table 4). Since the riverbed contains a high fraction of coarse sediments, samples were taken with spades with a depth between 5 and 15 cm along cross-sections.

Samples were dried at 40 °C up to 2 weeks. Then, samples were dry sieved using mesh sizes from 0.63 to 63 mm. Stones larger than 63 mm were individually weighted and measured by hand, measuring their length, width and depth (3 axis). In addition, all samples were divided into fine

fraction (diameters up to 0.063 mm) and coarse fraction (diameters between 0.063 and 63 mm) and Φ distributed after Krumbein and Pettijohn (1939). In addition, the skewness was computed according to Krumbein and Pettijohn (1939).

The grain size of the fine fraction up to 0.63 mm was measured with a Laser Diffraction Particle Size Analyzer (Beckman Coulter LS 13 320). Sediments were treated with 0.70 ml of 30% H_2O_2 at 70 °C to remove organic matter, and afterwards, with 1.25 ml $Na_4P_2O_7$ for 12 h on an overhead shaker (DIN ISO 11277; Pye & Blott, 2004). The Laser Diffraction Particle Size Analyzer calculates the frequency of grain sizes in 116 classes in percentage between 0.04 and 2000 µm with an error of 2%. The accuracy was increased by measuring four times with two different aliquots (Schulte et al., 2016). In addition, the fine fraction was analysed by XRF as described above in "Highly mobile sediment accumulations".

3.1.6 Type 3: Dam accumulations

Dam accumulations in the Urft reservoir and the auxiliary dam of the Rur dam were sampled and evaluated in former, respectively, parallel projects. Four bulk samples were taken in 2012 from the auxiliary dam of the Rur dam (cf. Figure 2) with a Van-Veen sampler in the upper 0.4 m (Henkel et al., 2012). Henkel et al. (2014) found, that sediments up to 2 mm were the main fraction deposited in the auxiliary dam of the Rur dam and, therefore, evaluated sampled sediments ≤ 2 mm with dry sieving. For geochemical analysis of the Urft reservoir and of the Rur dam (auxiliary dam) data from the DFG-Project "115 years of sedimentation in the Urft reservoir" was used, which was sampled with manual sediment core samplers (Stauch et al., 2021). Samples were collected near the dam and cores had lengths of about 4 m (Stauch et al., 2021).

In this work, vertical or horizontal variations of concentrations of dam sediments are not of interest. Here, only the minima and maxima are used to compare the concentration with the other sediment data sets. The treatment of sediment samples for XRF-analysis is the same as described above in "Highly mobile sediment accumulations".

3.2 Case study with Delft3D

Using the hydrodynamic modelling software Delft3D (Delft3D Flow, Version 4.04.01), we systematically investigate floodplain sedimentation caused by the Rur dam.

3.2.1 Model area

The model area covers two focus regions between the Rur dam and the Obermaubach basin (cf. Figure 3). Focus

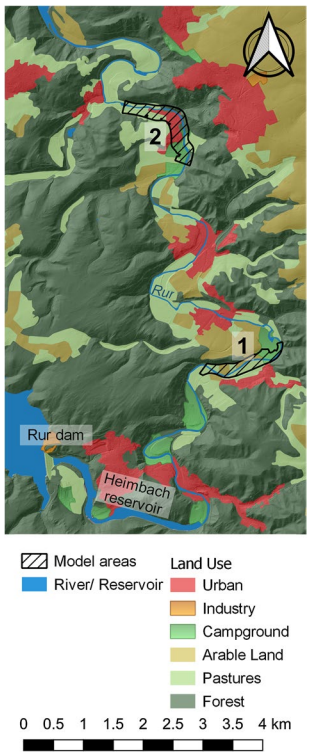

Fig. 3 Overview over model areas; own illustration; shading based on DEM25: (Bezirksregierung Köln, 2021), CLC land use data: (European Environment Agency, 2016), River course: (Geofabrik GmbH, 2018)

region 1 features a slightly sinuous 1.6 km long river section towards the uplands with floodplains used as pasture land. Focus region 2 covers 2 river-km further towards the lowlands (cf. Figure 3). Here, floodplains are settled or used as a campground and the river is partly regulated. Choosing two focus regions with different anthropogenic impacts on floodplains allows us to evaluate the spatial validity of the results obtained in the simulation. In Model 1, an area of 0.26 km^2 (without the riverbed itself) is covered by 4106 cells and in model 2, 0.39 km^2 (without the riverbed itself) is covered by 9150 cells. The models have a resolution of 2.5–18.5 m. Overall, the resolution is highest in the area of the riverbed and lowest towards the contours. Model 1 has a width of 220 m and model 2 has a width of about 300 m.

The model is based on an open-source DEM1 (digital elevation model with a resolution of 1 × 1 m) from data of image flights from 2019 (Bezirksregierung Köln, 2021). A uniform depth for the riverbed as well as the Q–H-outlet boundaries are based on cross sections measured and provided by the Bezirksregierung Köln (Bezirksregierung Köln, 2011). A uniform Chezy roughness of 31 $m^{1/2}/s$ is applied to the riverbed. Furthermore, critical shear stress for erosion $\tau_{erosion,bed}$ of 50 N/m^2 is applied to the channel, computed after Shields from the d_{50} of the complete sample, and

$\tau_{erosion,floodplain}$ of 17 N/m^2 is applied to the floodplains, computed after Shields from the d_{50} up to 63 mm. The critical shear stress, below which sedimentation starts, is 1000 N/m^2 for floodplains ($\tau_{deposition,floodplain}$) and 1 N/m^2 for the riverbed ($\tau_{deposition,bed}$). Values are in good agreement with Maaß and Schüttrumpf (2019b).

3.2.2 Scenarios

In three scenarios, the impacts of damming the Rur River are build up. As worked out in the background, large dams usually alter the discharge, cause a sediment deficit downstream and lead to a coarsening of the riverbed. First, conditions before dam constructions, hence, conditions without sediment deficit, are evaluated (scenario 1) (cf. Table 2). Afterwards, the situation after construction of the dams is evaluated (scenario 2) (cf. Table 2). After construction the dam, we assume that a sediment deficit immediately sets in. We further assume, that it takes a few years of adaption until the mean sediment diameter of the fine fraction increases in the dammed area and a new equilibrium has set up. This state of a new equilibrium incorporates today's parameters, including a deficit in the suspended sediment supply and an increased diameter in the fine fraction (scenario 3) (cf. Table 2).

3.2.3 Discharge input data

For generating inflow discharge data, for pre-dammed conditions, a tailored timeline, which is the sum of the inflow to the Rur reservoir and the inflow to the Urft reservoir is used covering 10 years, 2010–2020 (cf. Supplement B, Fig. 1a)). For dammed conditions, the actual discharge data of the Heimbach reservoir from 2010–2020 is used (cf. Supplement B, Fig. 1b)). From those time series, the minimal discharge, Q_{min}, the maximal discharge, Q_{max}, and the discharge at 75%-percentile, Q_{75}, are computed. Those characteristic discharges are the input data for the model, whereas Q_{min} and Q_{75} are applied for 3 months to represent a dry and a wet season, and Q_{max} are applied in form of a flood wave resp. a block discharge for regulated discharge conditions for a week (cf. Table 3).

Using an morphological scale factor of 800, the morphological impact of 800 times 3 months is computed (cf. Maaß & Schüttrumpf, 2018). Hence, the impact of Q_{min} and Q_{75} is evaluated over a morphological duration of 200 years. Furthermore, the impact of 800 accumulated flood events were modelled.

3.3 Sedimentological input data

A layer of sediments with the settling velocity characteristic for d_{50} of the fine fraction from the riverbed samples is applied to the simulation area. In addition, suspended sediment transport based on the samples taken from October 2019 to July 2021 are applied (cf. Figure 4). In scenario 1 conditions without a sediment deficit are resembled, and therefore, the value for the suspended sediment concentration measured at rkm 128, before the auxiliary dam. Furthermore, the settling velocity corresponds with the d_{50} of the fine fraction of sample 2 is computed after Cheng (1997). The settling velocity is 0.117 m/s in scenarios 1 and 2. As the results show, the d_{50} of the fine fraction increases from 0.013 mm to 0.014 between samples 2 and 3 and 0.022 for sample 4 (cf. Table 5). Therefore, a mean value of sample 3 and sample 4 is applied for computing the settling velocity

Table 2 Simulation scenarios in Delft3D

Scenario	Description	Inflow—discharge	Inflow–cohesive sediment	Cohesive sediment settling velocity determined by
1	Pre-dam conditions	Pre-dam discharge scenarios	No sediment deficit	Small mean sediment diameter
2	Impacts after dam closure; sediment deficit has set in	Post-dam discharge scenarios	Sediment deficit	Small mean sediment diameter
3	Today's situation; sediment deficit has set in; mean sediment diameter has increased	Post-dam discharge scenarios	Sediment deficit	Increased mean sediment diameter

Table 3 Model scenarios for discharge input data

Model discharge	Pre-dammed conditions	Regulated discharge	Model application
Q_{min} [m^3/s]	1.87	2.47	Constant over 3 months
Q_{75} [m^3/s]	15.28	10.20	Constant over 3 months
Q_{max} [m^3/s]	249.52	59.90	Flood peak over a week for pre-dammed conditions, block discharge over a week for dammed conditions;

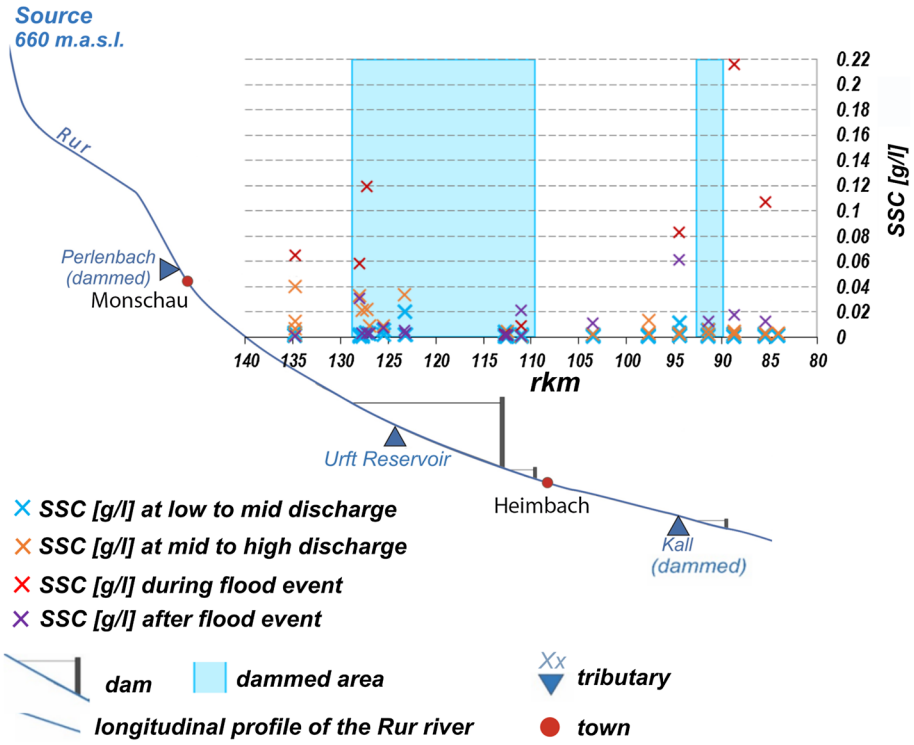

Fig. 4 Suspended sediment concentrations measured in the dammed section of the Rur River between October 2019 and February 2021, divided into samples taken at low to mid and mid to high discharge as well as during and shortly after a flood event mid July 2021

Table 4 Model values for the suspended sediment concentration

Model discharge	Model suspended sediment concentration [g/l] for		
	Pre-dammed conditions	Regulated discharge	Outlet
Q_{min}	0.00137	0.00131	0.00254
Q_{75}	0.00327	0.00203	0.00461
Q_{max}	0.0583	0.0114	0.0835

in scenario 3, which is 0.22 m/s. In scenarios 2 and 3 inflow concentrations are averaged from two sampling stations downstream of the Rur dam, at rkm 103.5 and 97.7. For the outlet condition, mean values from sampling sites at rkm 85.45 and rkm 84.1 are applied. Values for the sedimentological input data are shown in Table 4.

3.3.1 Data evaluation

The model results do not serve to determine an annual sediment growth rate, but to outline changes in sedimentation patterns due to the influences of damming on discharge data and sediment supply. Evaluated are the percentage of the floodplain and riverbank area affected by sedimentation as well as a mean height of sedimentation. By multiplying the percentage of the affected area with its mean height of sedimentation, an impact factor for sedimentation is generated. Sedimentation impact values on the floodplain and riverbanks are summed up for all three model scenarios (cf. Table 2). Afterwards, values are standardized in regard to scenario 1, pre-dammed conditions. With this, changes are expressed in percentage in comparison to pre-dammed conditions, since scenario 1 is assigned with the value 1.

4 Results

4.1 Suspended sediment transport

Overall, SSC at high discharge is higher than SSC at low discharge. The average SSC at low to mid discharge is 0.002 g/l and at mid to high discharge 0.009 g/l. During the flood event in mid of July 2021, suspended sediment concentrations were the highest in our data set, with an average value of 0.033 g/l (cf. Figure 4). The highest value was measured on July 15th, 2021 with 0.22 g/l downstream of the Obermaubach basin. The highest suspended sediment concentration besides the flood event in July 2021 was measured upstream of the dammed area at rkm 138.4 with 0.04 g/l (cf. Figure 4) during a mid to high discharge of 18.6 m^3/s. A week after the flood event, on July 22nd, 2021, discharge from the Rur dam was still very high with values around 60 m^3/s (Reichert, 2021). Suspended sediment concentrations on July 22nd, 2021 range around values of mid to high discharge upstream of the Rur dam, but are elevated downstream of the Rur dam with a maximum value of 0.061 g/l at rkm 94.45. The overall pattern shows a decline of SSC

towards the Rur dam, slowly increasing suspended sediment concentrations between the Rur dam and the Obermaubach basin, and again, lower values downstream of the Obermaubach basin. Therefore, the lowest concentrations, all below 0.002 g/l, were measured at rkm 111.05, downstream of the Rur dam (cf. Figure 4). Values downstream of the Heimbach reservoir at rkm 103.5 are the second lowest, except during the flood event.

4.2 Sedimentological riverbed composition

Grading curves of all eight sampling points include results from dry sieving and Laser Diffraction Particle Size Analysis (Fig. 5). Samples in the uplands are represented with black curves, and samples in the lowlands are represented with grey curves. On all eight sampling points, the Rur River is dominated by coarse sediments with fine fractions of less than 1%. Samples 1, 3, and 4 are the coarsest, sample 8 is the finest and especially high in medium-sized gravel in comparison to all the other seven samples. The grading curves of all samples have similar shapes, except for sample 8, due to its comparably high fraction of medium gravel and sample 1, which contains a high fraction of boulders. However, a strict displacement downstream with samples becoming consistently finer is not observed. Instead, sample 2 is significantly shifted to the finer, and sample 5 is significantly shifted towards the coarser (cf. Figure 5).

In the dammed area, a clear shift in the retained sediments in the auxiliary dam from coarse to fine can be observed (cf. Figure 6). First, at sampling site A, the sedimented sediments contain of over 90% of sand. Close to the dam (sample D), the sample contains of about 95% of clay and silt. However, the retained sediments in the auxiliary dam are not a mayor part of the whole sediment spectrum in the riverbed upstream and downstream of the Rur dam, since this sediment fraction roughly makes 5% of the riverbed sediments.

Since the fine fraction is so small, the fractions from 0 to 63 µm, and the fraction from 63 µm to 63 mm are observed separately. The fine fraction is suited to give an insight in the sediment deficit caused by the dam and the coarser fraction is suited to look at general shifts of the grading curve and effects, such as bed armouring. In addition, the fine fraction, 0–63 µm is evaluated separately, since this fraction most likely is transported in suspension.

Upstream of the Rur dam, the mean sediment diameter of the sediment fraction between 0 and 0.063 mm is 0.015 mm in the uplands at sampling point 1, and 0.013 mm at sampling point 2, where floodplains are wider. The mean sediment diameter of the sediment fraction between 0 and 2 mm is 0.940 mm at sampling point 1 and 0.940 mm at sampling point 2. Downstream of the Rur dam, the mean sediment diameter of the sediment fraction between 0 and 0.063 mm changes to 0.014 mm (sample 3) and 0.022 mm (sample 4).

The fine fraction as Φ-distributed grading curve shows, that samples from sampling points 2 and 3, right before and right after the Rur dam, contain the highest silt fractions (cf. Figure 7). In addition, they are almost linear, while grading curves from sampling points 4, 5, 6, 7, and 8 show a convex shape. The grading curve from sampling point 1 shows a high fraction of coarser silt.

The grading curve of sample 8 shows a high fraction of mid to coarse gravel (cf. Figure 8). In addition, sample 8

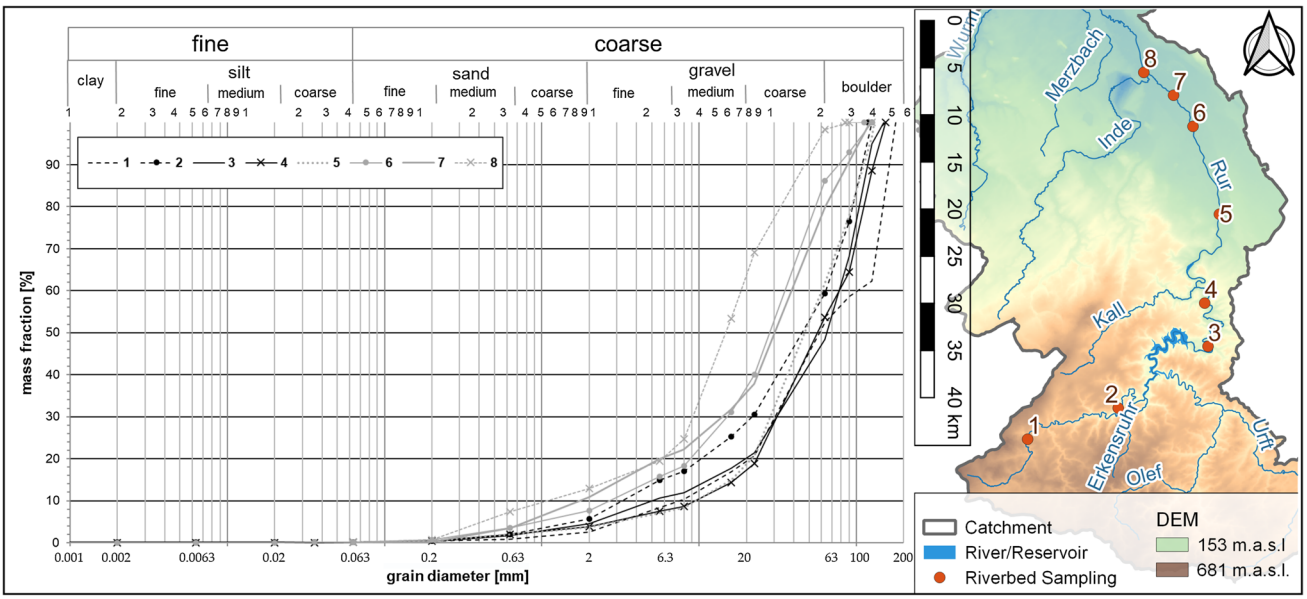

Fig. 5 Grading curves of riverbed samples

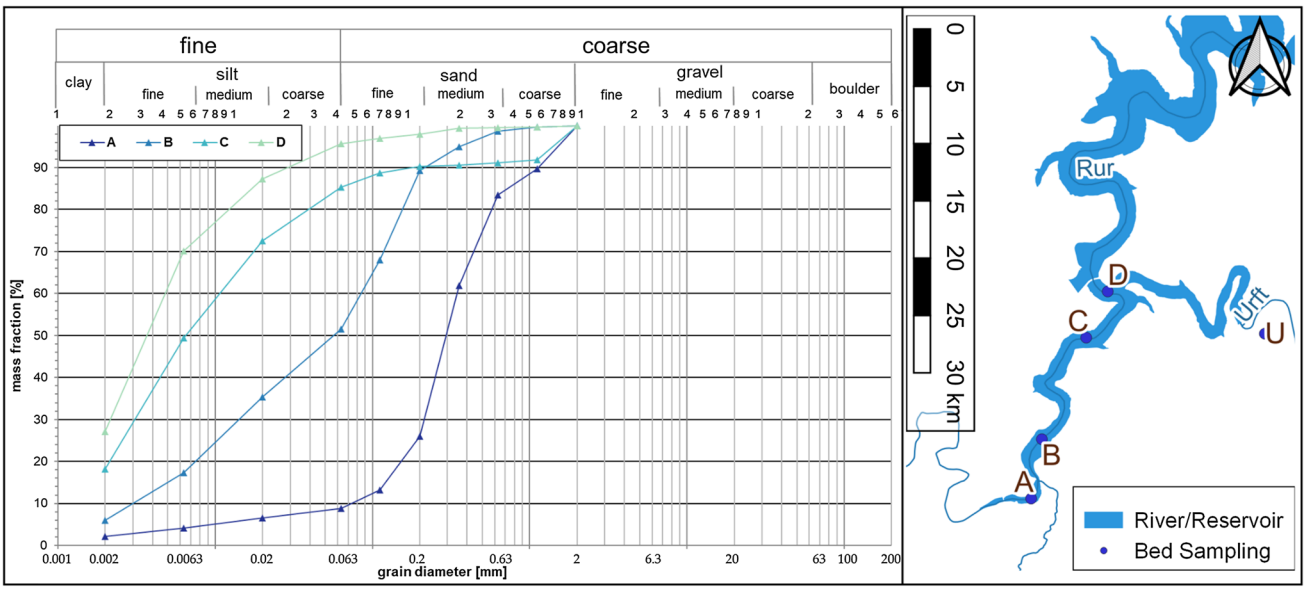

Fig. 6 Grading curves of riverbed samples before and after the Rur dam and grading curves of bed samples taken from the auxiliary dam in 2012

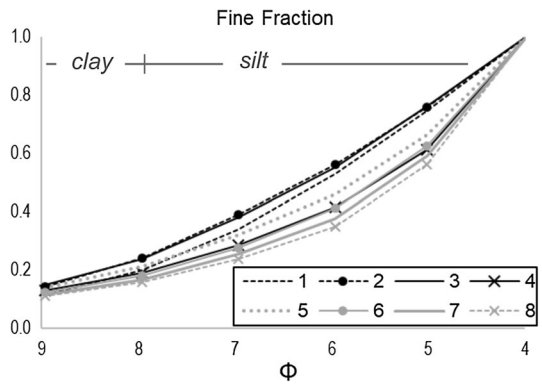

Fig. 7 Φ-Distribution of sediments ≤ 63 µm, consisting silt and clay

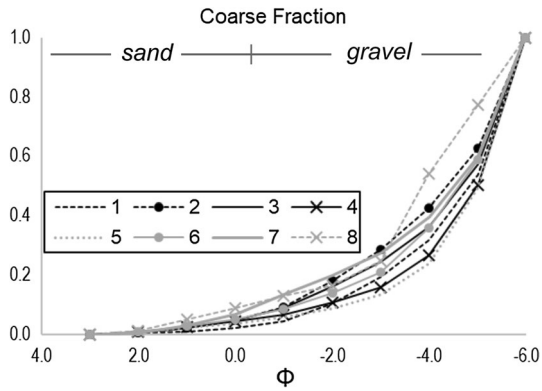

Fig. 8 Φ-Distribution of sediments ≥ 63 µm up to 63 mm, consisting sand and gravel

contains slightly higher amounts of sand, compared to the other grading curves. Sample 1 shows the lowest sand fraction. The riverbed samples from the sampling points 4 and 5, before and after the Obermaubach basin, are the coarsest. Samples 2, 7, and 8 are relatively fine in comparison to the other samples.

Table 5 shows the mean diameter of the samples as well as statistical parameters according to Krumbein and Pettijohn (1939). The mean diameter of the whole sample contains hand-measured cobbles as well. The diameter of all fractions ≤ 63 mm contains sieved and laser-measured fractions. Comparing the d_{50} of the whole sample, overall, the diameter declines, except for an interim increase between the Rur dam and the Obermaubach basin (samples 3 and 4). The d_{50} of the sediments ≤ 63 mm show a similar development. However, the fine fraction is showing an increase in d_{50} from sample 1 to sample 8. The Φ_{50} of the fine fraction shows a coarsening from sample 1 to sample 8 as well. Results are comparable as expected, since d_{50} and Φ_{50} can be converted into each other.

The skewness of samples was computed using Φ_{25} (respectively, Q_1), Φ_{50}, and Φ_{75} (respectively, Q_3), according to Krumbein and Pettijohn (1939) (cf. Table 5). Overall, the skewness (Sk) of all samples ranges from 0.70 (sampling point 7) to 0.99 (sampling point 8) and does not follow a clear pattern. Upstream of the dam, sediments have a skewness of 0.80 (sample 1) and 0.74 (sample 2). Sediments downstream of the dam, have a skewness of 0.76 at sampling point 3 and 0.85 at sampling point 4. Downstream of the Obermaubach basin (sampling point 5), sediments have a skewness of 0.88. In the lowlands, at sampling points 6 and

Table 5 Mean diameters of riverbed samples

Sample	d_{50} [mm]			Φ_{50}		Q_1	Q_3	Sk
	Whole sample	≤ 63 mm	Fine fraction	Fine fraction ≤ 63 µm	Coarse fraction ≤ 63 mm	≤ 63 mm, according to Krumbein and Pettijohn (1939)		
1	59.9	29.4	0.017	6.1	−4.8	−3.4	−5.4	0.80
2	49.9	21.3	0.016	6.3	−4.4	−2.6	−5.3	0.74
3	63.1	26.5	0.016	6.3	−4.6	−3.0	−5.4	0.76
4	58.7	31.7	0.031	5.6	−5.0	−3.8	−5.5	0.85
5	51.4	32.5	0.024	5.8	−5.0	−4.0	−5.5	0.88
6	31.1	25.0	0.028	5.6	−4.6	−3.2	−5.4	0.83
7	34.1	24.4	0.030	5.4	−4.5	−2.6	−5.4	0.70
8	15.0	14.8	0.036	5.3	−3.9	−3.0	−4.9	0.99

7, sediments have a skewness of 0.83 and 0.70, whereas downstream of the Inde River tributary, sediments have a skewness of 0.99.

4.3 Sediment-bound pollution transport

Figure 9 shows Cu- and Pb-concentrations of different sediment samples along the Rur River. Pb and Cu concentrations follow a similar pattern; the lowest value ranges upstream of the Rur reservoir, higher concentrations in retained sediments in the Urft reservoir, increased concentrations in floodplain sediments downstream of the Obemaubach basin, and decreasing values further downstream.

Upstream of the valley Monschau (rkm 151.5 and 147.6), Pb concentration of riverbed sediments, varies between 67.7 and 153.4 mg/kg. Downstream of the village Monschau, the value range of Pb concentrations from riverbed sediments, grading curves and flood sediments lies between 96.8 and 214.2 mg/kg, while the value range of floodplain sediments (depth profiles) lies between 19.9 and 25.9 mg/kg. The Cu values of all samples increase slightly as well between the sampling site at rkm 151.5 and 128.0 (values between 17.1 and 61.5 mg/kg).

The min-value (87.4 mg/kg for Pb, 37.7 mg/kg for Cu) and max-value (178 mg/kg for Pb, 70.7 mg/kg for Cu) of sediments taken in the auxiliary dam represent the value range of almost all sediment samples from upstream. However, the max-value of the Urft reservoir sediments is with 1153 mg/kg the highest value of this data set for Pb, and shows an elevated concentration for Cu with 125.9 mg/kg. Between the Rur reservoir and the Obermaubach basin the Pb concentrations of riverbed sediments, grading curve sediments, and flood sediments range between 105.4 and 367.5 mg/kg. The grading curve sediments at rkm 108.1 show with 155.7 mg/kg higher Cu concentration than the riverbed sediments, grading curve sediments, and flood

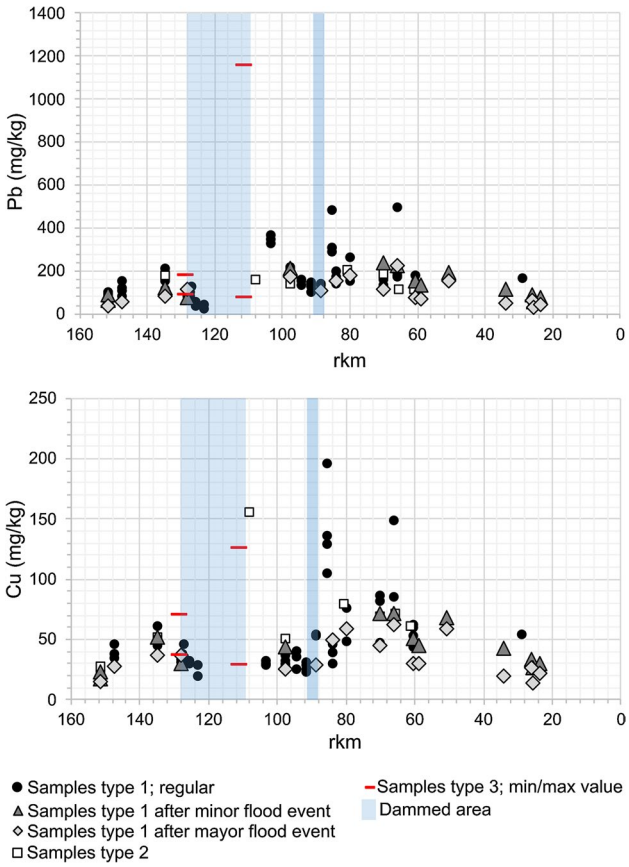

Fig. 9 Longitudinal profile of Pb and Cu concentrations along the Rur River based on different sampling methods

sediments between rkm 103.5 and Obermaubach basin (23.1–51.4 mg/kg).

Downstream of the last reservoir, Obermaubach basin, the Pb concentration values of riverbed sediments (104.5–496.4 mg/kg), grading curve sediments (112.6–208.2 mg/kg) and flood sediments (58.5–240.4 mg/kg) are more elevated compared to the upper reach of the

river. Downstream of the Obermaubach basin to rkm 66, the riverbed sediments vary between 38.9 and 196.8 mg/kg for Cu, whereas the contents of the grading curve sediments and flood sediments in these river reaches vary between 69.1 and 80 mg/kg. By trend, flood sediments show slightly decreasing values with increasing flow path (value range 26.4–68.1 mg/kg).

4.4 Numerical case study

A graphical presentation of floodplain sedimentation in model area 1 and model area 2 is presented in the supplement, in Supplement C, Figs. 2 and 4. In addition, water depths for the three discharge scenarios are provided (cf. Supplement C, Figs. 3 and 5).

Sedimentation is evaluated on the floodplains and on the riverbanks in both model areas (cf. Table 6). In pre-dammed conditions (scenario 1), areas of sedimentation, as well as the mean sedimentation rate are at its highest in both model areas. Both parameters decline with dam construction (scenario 2) and the area of floodplain sedimentation is on its lowest in today's scenario (scenario 3). However, in scenario 3, the mean sedimentation rate is slightly higher than in scenario 2. Sedimentation is higher with higher discharges. In addition, the area affected by sedimentation as well as the sedimentation rate are higher in model area 1 than in model area 2.

Table 6 Sedimentation on floodplains and riverbanks in model 1 and model 2 in three different scenarios for Q_{min}, Q_{75} and flood event

Floodplain and riverbank sedimentation				
	Scenario	1	2	3
Q_{min}				
Modell 1	area [%]	1.7	1.6	0.5
	mean [cm]	2	2	5
Modell 2	area [%]	0.8	0.8	0.7
	mean [cm]	6	6	8
Q_{75}				
Modell 1	area [%]	2.1	1.8	0.6
	mean [cm]	4	2	4
Modell 2	area [%]	0.7	0.5	0.5
	mean [cm]	25	10	13
Flood				
Modell 1	area [%]	46.3	16.8	14.6
	mean [cm]	257	13	21
Modell 2	area [%]	15.9	1.5	1.5
	mean [cm]	60	10	14
Explanation		Pre-dammed condition	Shortly after dam construction	Today's scenario

Results for 200 years of discharge event or 800 flood events

Figure 10 shows the standardized changes for floodplain sedimentation which's origin is described in Sect. "Case Study with Delft3D, Data Evaluation". Sediment accumulation on floodplains and on riverbanks is reduced after dam closure (cf. Figure 10). In model area 1, after dam closing (scenario 2), sedimentation drops to 1.9% if pre-dammed conditions in model area 1 and 2.6% of pre-dammed conditions in model area 2. After the d_{50} of the fine fraction has increased (scenario 3), floodplain sedimentation increases to 2.6% of pre-dammed conditions in model area 1 and 3.4% in model area 2.

5 Discussion

5.1 Influence of dams on suspended sediment and pollutant transport

As expected, the suspended sediment concentration in the Rur River is higher at higher discharges with an average of 0.009 g/l at mid to high discharge and 0.033 g/l at the flood event in July 2021. This general relation between discharge and suspended sediment transport is well known for decades (e.g., Ferguson, 1986, McBean & Al-Nassri, 1988; Walling, 1977). In addition, we can see a reduction in suspended sediments downstream of the Rur dam, as expected in comparison to various other dams (e.g., Pal, 2016, Walling, 2012, Williams & Wolman, 1984; Yang et al., 2014, Pal, 2016). The behaviour of the suspended sediment concentration along the Rur River is similar for low to mid and for mid to high discharge (cf. Figure 4). During the flood event in mid-July 2021; however, we measured an increased suspension load downstream of the Obermaubach reservoir. We believe, that the increased values are caused by the high

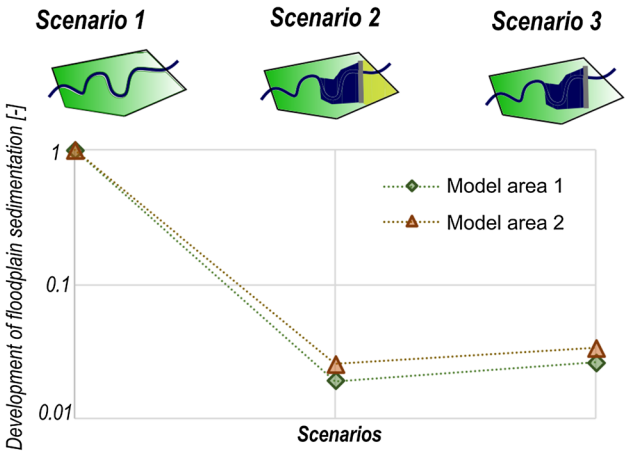

Fig. 10 Change of sedimentation on the floodplains and riverbanks after dam closure (scenario 2) and after new equilibrium has formed (scenario 3) in comparison to pre-dammed conditions (scenario 1)

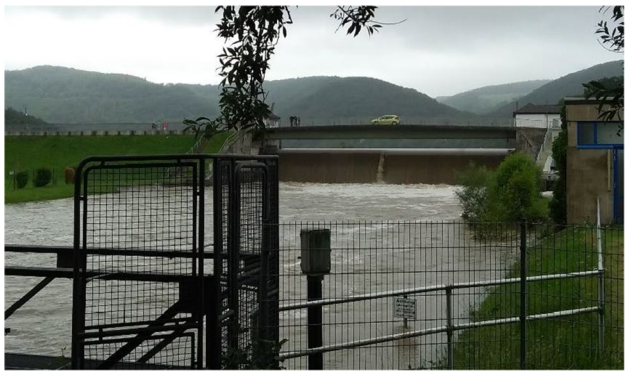

Fig. 11 Overflow over the tilting weir at the Obermaubach basin on July 15th 2021, picture was taken while collecting water samples for SSC measurements (Verena Esser, 2021)

amounts of flotsam, which accumulated at the tilting weir. The water samples were collected when the weir was overflowing (cf. Figure 11). The Obermaubach basin, which can hold a water volume of 1.65 Mio m^3 (Wasserverband Eifel-Rur, 2017c), is significantly smaller than the Rurtalsperre Schwammenauel, which can store 202.6 Mio m^3 (Wasserverband Eifel-Rur, 2017a) and an additional 1.12 Mio m^3 in the Heimbach reservoir (Wasserverband Eifel-Rur, 2017b). In addition, the Obermaubach basin is located in a stretched valley, whereas the Rur reservoir is located in a sinuous valley. Consequently, in the Obermaubach basin, organic components as drifting materials were accumulated on the reservoir's surface close to the dam in a higher extent than in the Schwammenauel basin or the Heimbach reservoir. The accumulations increased the suspended matter concentration in the spillover of the dam. In addition, riverbank sediments, which are usually not affected by the flow, were mobilized due to high water levels downstream of the dam. In addition, we assume, that sediment settling in the reservoir itself was reduced due to the draining. Bi et al., 2014 in Ciszewski and Grygar (2016) found that sediments are easily re-suspended during water release from reservoirs, and Walling (1977) stressed that organic matter does play an important role in the SSC. The spillway of the Rur dam, however, was hardly activated with only 20 m^3/s (Reichert, 2021). Therefore, the Rur dam still caused a sediment deficit during the flood event in mid-July 2021, as we can see in our data.

Furthermore, during the flood event, concentrations of suspended sediments increased upstream of the backwater of the Obermaubach basin. In this area, the Kall River flows into the Rur river. During fieldtrips, we often observed higher turbidity in the water of the Kall River in comparison to the Rur river. Hence, it is likely, that activation of the subcatchment by the flood event can be observed in the SSC-Data. The Kall River is a coarse material-rich, siliceous low mountain stream with some agricultural land use in its rather steep valley and it is common for those tributaries to be a sediment source for receiving waters with wider river valleys (Bogaart et al., 2002), as the Rur river is in this section. Nevertheless, as the results show (cf. Figure 4), suspended sediment concentrations are generally higher upstream of the Rur reservoir than in the section between the Rur dam and the Obermaubach basin (Fig. 12).

The natural concentration of sediment-bound trace elements such as Cu or Pb depends on the geological setting. Thus, regions with ore deposits have in general higher natural background concentrations. River catchments with diverse geological realities, such as the Rur catchment, can show variations. The value ranges of Pb and Cu concentrations at the auxiliary dam represent the concentrations measured in almost all riverbed sediments collected upstream, which include natural background concentrations (Szarek-Gwiazda et al., 2011) and anthropogenic impact, e.g., of the textile industry in Monschau. This indicates that the recent sediment transport affects and controls the value ranges of Cu and Pb of auxiliary dam sediments. Nevertheless, it might be that the changes in grain size between the beginning of the backwater zone and the dam (Ziegler & Nisbet, 1995) may influence the concentrations (Sojka et al., 2019; Zhao et al., 2013).

Tributaries such as the Urft River can play an important role as source regions for pollutants, especially in mining areas (Schintu et al., 1991). The value ranges of the Urft sediments are the highest between the source of the Rur River and the inflow of the Urft River, caused by historical Pb- and Cu-ore mining and its processing (Blass & Graf, 1995; Weiss, 1990a). For Pb, the reservoir sediments show the highest concentrations of the whole data set (1153 mg/kg), which shows, that each reservoir carries its characteristics

Fig. 12 Differences in turbidity between the Kall River (tributary) on the right and tis receiving water, the Rur River (on the left) on dd.mm.2021 after a rainfall event (Verena Esser 2021)

of pollutant fingerprints (Sojka et al., 2019). Decreasing concentrations of riverbed sediments between the two dams and the subsequent anthropogenic pollution sources show retention of contaminated sediments (Bi et al., 2014; Palanques et al., 2014), which verifies a disruption of sediment transport. This interruption correlates with the reduced SSC downstream of the Rur dam (cf. Figure 4), since the suspended sediment transport is closely linked to sediment-bound pollution transport. At the Rur River, the next detectable source is historical Cu-, Pb, and Zn-ore mining next to the villages of Leversbach (pit Aurora) and the village Horm (pit Maubacher Bleiberg) (Weiss, 1990b). In these areas, small creeks draining the mining sites may play an important role in the input of heavy metals (Schintu et al., 1991).

5.2 Influence of dams on riverbed composition

Since the Rur River is dominated by coarse fractions and only transports a small part of its sediment as suspended load, the fine fraction, $d < 63$ µm, and the fraction $d > 63$ µm are evaluated separately (cf. Figure 13). On one hand, we see a sediment deficit, concerning the fine fraction, downstream of the Rur dam in our data (cf. Figure 4), but on the other hand, East et al. (2015) found changes in sediment composition up to cobble and boulder size after the removal of the Elwha dam in Washington, USA. Therefore, both, the fine and the coarse fraction of the riverbed seem to be affected by damming. Since smaller Φ-values correspond to larger particle diameters, slight coarsening in the fine fraction after dammed areas can be observed. This result is already used for the input data for Delft3D and is a common phenomenon

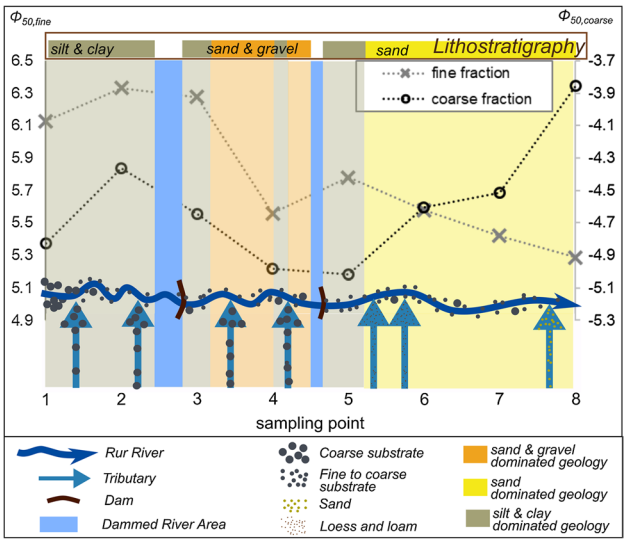

Fig. 13 Development of Φ_{50} of the fine and coarse fraction of riverbed samples in relation to the rivers background lithostratigraphy and tributaries as sediment sources

of dams (Williams and Wolman 1984). Overall, the fine fraction shows only small changes. However, the change in the fine fraction from $\Phi_{50,\text{fine}} = 6.1$ to $\Phi_{50,\text{fine}} = 5.3$ between sampling points 1 and 8 do not show the typical effect of downstream fining along a river, whereas the change in the coarser fraction from $\Phi_{50,\text{coarse}} = -4.8$ to $\Phi_{50,\text{coarse}} = -3.9$ does (cf. Table 5, Fig. 13). Those developments can only be explained in the context of sedimentology and adding tributaries (cf. Figure 13, see Supplement D, Fig. 6 for classification of the tributaries). Contradictory, the gates of the Saint-Sauveur dam on the Buëche River in southern France enable higher sediment loads to pass during flood events, but due to sedimentation of coarser fractions in the backwater zone, a sediment deficit, especially in coarser fractions downstream exist nevertheless (Brousse et al., 2020). Even though the direct impact of the Rur dam and the Saint-Sauveur dam are different, both impacts can only be observed over a short downstream reach (Brousse et al., 2020).

The uplands are dominated by clay-slate (Elfers), which is easy to erode. This causes high fine fractions besides very large cobbles in the riverbed. Therefore, although the fine fraction at sampling point 1, $\Phi = 9$ up to $\Phi = 4$, makes up a very small fraction of the riverbed (cf. Figure 8), it contains of over 20% of clay (cf. Figure 7). Accordingly, the Φ_{50} of the coarser fraction is rather small with $\Phi_{50,\text{coarse}} = -4.8$ (cf. Table 5, Fig. 13). Both samples taken upstream of the dammed area show higher clay and fine silt contents. Therefore, the cohesive fractions are larger in samples taken upstream of the dam (cf. Figure 7). The grading curves of the fine fraction of samples taken in the uplands (samples 1–4) have a lower slope in the cumulative curve of their fine fraction, than samples 5–8 (cf. Figure 5), which means, that they are better sorted (Weller, 1988). According to Weller (1988), fossil sediments have higher suspended sediment fractions which are rather poorly sorted. In addition, the slope of the Rur River decreases towards the Rur dam and the valley becomes wider leading to a more sinuous course (cf. Supplement A, Table 4). Hence, particle diameters decrease due to the reduced flow velocity. Downstream of the Rur dam, at sampling sites 3 and 4, particle diameters increase, probably due to the overlapping of the trapping effect by the Rur dam with the change in lithostratigraphy from mostly silt and clay embossed to sand and gravel embossed. In addition, two tributaries rich in coarse materials function as a sediment source. Downstream of the Obermaubach basin, at sampling site 5, the Φ_{50} of the fine fraction increases due to the change in background lithostratigraphy to silt and clay dominated. In addition, the valley becomes wider at sampling site 5, and flow velocities decrease in comparison to sampling site 4 (cf. Supplement A, Table 4). In addition, the area becomes more urban and agriculturally influenced, which leads to increased fine sediment input into the river (e.g., Panagos et al., 2020; Szatten & Habel, 2020). The Φ_{50} of the coarse

fraction, however, slightly increases. The very small change could be caused by inaccuracies or due to the formation of gravel bars in the comparatively wide riverbed.

Towards the lowlands, downstream of the Obermaubach basin, an increase in fine material can be observed in the Rur River, corresponding with tributaries rich in loess and loam (cf. Figure 13).

Downstream of sampling site 5, two loess and loam dominated lowland streams, flow into the Rur River, probably leading to the steady decrease of the Φ_{50} of the fine fraction in sampling sites 6, 7, and 8, besides the sand dominated geological background. In addition, the sand-prone Inde River flows through the agricultural-dominated area and carries, therefore, higher fractions of silt, which could explain the further decrease of the Φ_{50} of the fine fraction. However, the Φ_{50} of the coarse fraction decreases due to the sand embossed geological background and the inflow of the Inde River. Overall, the findings agree Frings (2004), who found that tributaries with high sand input into receiving waters lead to significant coarsening.

When looking at the skewness of the samples (cf. Table 5), sediments from sampling sites 2, 3, and 7 show similar values to glacial till, since they have a skewness of 0.74, 0.76, and 0.70, whereas 0.75 is characteristic for glacial till (Krumbein & Pettijohn, 1939). Sediments from sampling sites 1, 4, 5, and 6 have a skewness of 0.8, 0.85, 0.88, and 0.83, which means that they are shifted towards coarser sediments. Sediments from sampling site 8 have the same skewness as beach gravel, being 0.99 (Krumbein & Pettijohn, 1939).

The skewness of the samples upstream of the Rur dam very likely shows values characteristic of glacial tilt, since the sediment composition of the lower rhine embayment was influenced by the last permafrost in the late Pleistocene, resulting in the 3rd main terrace (Boenigk, 1978). Especially in the low mountain area, rivers are incised in a Paleozoic gravel embossed bedrock, whereas floodplains are dominated by deposited brown soil and gley, which have a finer granularity (Lehmkuhl, 2011). The high fraction in coarse-grained materials and larger stones were probably derived from the Meuse catchment during the Pleistocene (Westerhoff et al., 2008).

Downstream of the Rur dam the skewness is increased compared to upstream and the grain size distributions are shifted to the coarser (cf. Figure 6), which is characteristic of bed armouring (cf. Sutherland, 1987). In addition, a change to a more "S-shaped" distribution is common with bed armouring (Sutherland, 1987). We cannot see the significant "S-shaped" cumulative curve typical for bed armouring (Sutherland, 1987) (cf. Figures 6, 7, 8); however, both the fine fraction and the coarse fraction become more concave, which tends towards a "S-shape". Therefore, the sediment deficit through damming as well as the flow alterations leading to uniform flow over longer periods seem to have caused bed armouring downstream of the Rur dam.

Overall, the main driver for changes in the riverbed composition is a strong geological impact caused by valley shapes, the background sedimentology, and the inflow of tributaries with different river types. Our findings confirm the findings of Milliman and Syvitski (1992) who state that topographic relief, sediment erodibility, depending on lithostratigraphy and land use, are the main drivers for sediment transport. In addition, Ziliani and Surian (2012) found that the sediment deficit caused by numerous check dams on the Tagliamento River, a large gravel-bed river in northeastern Italy, was equalized by local hillside erosion and, therefore, had almost no morphological impact. The second most important impact seems to be the flow alteration together with the sediment deficit. Since usually sediment is not transported directly through the rivers into the ocean, but the majority finds its sink within the river system (Walling, 2012), they, therefore, have its source within the river system as well. Accordingly, Collins et al. (1997) state that surface erosion in a sub-basin may be the most important source of fine sediment in the water body. Hence, at least for typical European rivers, we assume, that the sediment deficit has a short sphere of action. Hence, in our case, it can be assumed, that anthropogenic impact is overlaid by natural factors.

5.3 Influence of discharge regulations on morphodynamical river development

Results from the numerical case study with Delft3D show, that floodplain sedimentation is drastically decreased after dam construction (cf. Figure 10). After the dam construction, the mean sediment diameter of the fine fraction increases due to coarsening effects described in the background and shown in our data. The impact of sediment coarsening is evaluated in the comparison between results from scenario 2 and scenario 3. Here, floodplain sedimentation increases again, but by less than 1%. For model area 1 and model area 2 this development is the same and almost identical factors for sedimentation development were obtained (Fig. 10). Hence, the discharge regulation by the dam causes the highest impact on downstream morphology. The Siemianówka Reservoir also significantly changed the flow regime of the coarse-material-rich Narew River, which will probably impact the riparian vegetation and lead to a reduction of anabranches downstream of the reservoir (Marcinkowski & Grygoruk, 2017).

High discharge is connected with a higher sediment supply, which was considered in our model by coupling discharge and sediment input data. As our results show, dam construction leads to a significant reduction in floodplain sedimentation. Our results are confirmed by Maaß and Schüttrumpf (2019b), who describe floodplain

decoupling in relation to mill weirs on the Wurm River, a main tributary of the Rur river. Floodplain decoupling in connection with discharge regulation in the Rur catchment was also detected by Lehmkuhl (2011), who additionally described the loss of soil types of bog gleys and fens, which are fertile soil types (Benke et al.). Bunte (2004) describes floodplain decoupling after the construction of hydroelectric dams in gravel embossed rivers as well. As a consequence of reduced floodplain flooding, hardwood develops and leads to increased riverbank stabilisation, which hinders the sediment availability within the stream (Bunte 2004).

Reduced flooding was one of the main goals of river regulation on the Rur River (Paul, 1994, 1999) and one of several goals for dam construction (Franzius & Proetel, 1927). Decoupling of floodplains occurs independently of the topological characteristics of the two model areas. Model area 1 has lower floodplains, and therefore, wider areas are affected by flooding and sediment deposition than in model area 2 (cf. Supplement C, Figs. 2, 3, 4). Maaß and Schüttrumpf (2019b) and Maaß and Schüttrumpf (2018) concluded as well, that greater flood events led to higher sedimentation rates on floodplains. The highest sedimentation rates are detected closer to the riverbed, which agrees with Maaß and Schüttrumpf (2019a), who found that sedimentation rates on floodplains are highest close to the river's channel. When sediment coarsening sets in (scenario 3), sedimentation slightly increases again, but affected areas decrease. Since an increased sediment diameter leads to a higher settling velocity, it can be assumed, that larger amounts of sediments settle earlier, leading to slightly higher accumulations. Overall, we assume, that the sediment deficit caused by the dam is quickly balanced out by local sediment supply and tributaries. Furthermore, the regulation of high flood evens leads to floodplain decoupling, probably over the complete reach from the Heimbach reservoir to the Obermaubach basin.

In addition, the Rur dam has a high storage capacity and can buffer large flood events. As we could observe in our SSC-Data (cf. Figure 4), the Obermaubach basin, which is significantly smaller, behaved differently from the Rur reservoir. Hence, a comparison of smaller and larger dams would be interesting, either within the catchment of the Rur River itself, which holds several smaller reservoirs, or worldwide. Nevertheless, it can be assumed, that floodplain decoupling is the main impact of dams of different sizes on rivers rich in coarse materials, since Maaß and Schüttrumpf (2019b) obtained similar results for mill dams. Hence, the impact of dams on downstream reaches in coarse-material-rich rivers seems to be similar on micro- and meso-catchment scale, as they are described in Maaß et al. (2021).

6 Conclusions

In this study, the morphological impact of the Rur dam, as model example for a large dam in a European low mountain area on the transition area to the lowlands, was evaluated by a hybrid examination of field measurements and numerical modelling using Delft3D. Field studies included sampling of three different types: short-time transported sediments, including fine sediments from the riverbed, floodplains, and suspended sediment samples (type 1), riverbed samples evaluating the current riverbed composition (type 2), and samples of dam accumulations (type 3). Results from the sediment studies were incorporated into the numerical model, which investigates the effects of discharge regulation, sediment deficit, and an increased sediment diameter in two model areas downstream of the Rur dam. Discharge data for the last 10 years was evaluated to determine the effect of discharge regulation caused by the Rur dam. Pollutant transport along the Rur River was evaluated from samples type 1 and type 2.

Dam construction on the Rur river started in 1900 and today, a new equilibrium incorporating flow regulations, a deficit in the suspended sediment supply, and an increased diameter in the fine fraction has set in. In addition, the Rur catchment holds a long history of industrial development and mining, which leaves various sources for heavy metal pollutants up to today. Since those pollutants are sediment-bound transported, they can function as markers for morphodynamical development.

The main findings of this study are:

- Field data shows a coarsening of the riverbed, as well as a reduction in the SSC downstream of the Rur dam. Hence, the impact of sediment retention is of interest even for coarse-material-rich river types.
- However, local lithostratigraphy and tributaries are an important sediment source, which balances out the sediment deficit caused by damming.
- The numerical model shows that the impact of the increased mean sediment diameter as well as the reduction in the SSC is very small compared to the impact of flow regulation by the Rur dam.
- Reduced flood events caused by discharge regulations through damming leads to floodplain decoupling downstream of the dam.
- Pollutant profiles along a river are highly dependent on local sources and therefore, the impact of a dammed area can be covered by downstream sources. For the Rur River, the reservoir functions as a pollutant trap, which is beneficial for the downstream reach.

Our results are specific for a large dam on a river rich in coarse sediments in a low mountain area and the transition region to lowlands. The influence of a large dam highly depends on the riverbed composite and the local lithostratigraphy. Therefore, the sediment deficit caused by a dam can have a much more significant impact on downstream river morphology for different river types. A national and international comparison of smaller and larger dams would be interesting, since we expect smaller reservoirs to respond differently, especially during flood events. Overall, more studies on the impact of damming on downstream reaches incorporating field data as well as numerical modelling are needed to classify the impact depending on the river type. Knowledge of the impact of damming on the downstream reach is crucial for sustainable water management.

Supplementary Information The online version contains supplementary material available at https://doi.org/10.1007/s43217-022-00103-9.

Acknowledgements We would like to thank Carole Detampel, Dymphna Maybelle Kroll, Christian Vogelgesang, Mariam Tsitsagi, Christina Schwanen, Maximilian Formen, Thomas Schröder, Mariela Bregu, Fabian Schmiedecke, Nima Garkazi and Valentin Kühn for participating in field and laboratory work. We also would like to thank Mrs Lehmkuhl and David Stenger for helping us taking samples. In addition, we would like to thank Anna-Lisa Maas and Jan Oetjen for their highly appreciated advice regarding the numerical modelling. We further would like to thank Christof Homann (WVER), Friedhelm Hackert (LANUV) and Lars Pleva (Bezirksregierung Köln) for providing us with hydraulic data.

Author contributions SW and VE wrote the first draft of the manuscript. All authors contributed to specific aspects of the manuscript. All authors read and approved the final manuscript.

Funding Open Access funding enabled and organized by Projekt DEAL. Open Access funding enabled and organized by Project DEAL. This work is funded by the Deutsche Forschungsgemeinschaft (DFG)—under project number 418362535.

Availability of data and materials Not applicable.

Code availability Not applicable.

Declarations

Conflicts of interest The authors declare, that no conflicts of interest exist.

References

Adib, A., Foladfar, H., & Roozy, A. (2016). Role of construction of large dams on river morphology (case study: The Karkheh dam in Iran). *Arabian Journal of Geosciences*. https://doi.org/10.1007/s12517-016-2693-2

Anderson, M. G. (Ed.). (1996). *Floodplain processes*. Wiley.

Annandale, G. (2013). *Quenching the thirst: Sustainable water supply and climate change*. CreateSpace Independent Publ.

Assani, A. A., & Petit, F. (2004). Impact of hydroelectric power releases on the morphology and sedimentology of the bed of the Warche River (Belgium). *Earth Surface Processes and Landforms, 29*, 133–143. https://doi.org/10.1002/esp.1004

Beaumont, P. (1983). Water resource management in the USA: A case study of large dams. *Applied Geography, 3*, 259–275. https://doi.org/10.1016/0143-6228(83)90045-0

Benke, M., Kaiser, M., Buchen, C., Well, R., Helfrich, M., Gensior, A., Fliessa, H. Auswirkungen von Grünlanderneuerung und Grünlandumbruch auf N-Verluste und Erträge. Nachhaltige Milchproduktion: Forschung und Praxis im Dialog:67

Bezirksregierung Köln. (2011). *Hochwasseraktionsplan Rur Querprofile*

Bezirksregierung Köln. (2021). *Digitales Geländemodell*. https://www.bezreg-koeln.nrw.de/brk_internet/geobasis/hoehenmodelle/digitale_gelaendemodelle/gelaendemodell/index.html. Accessed 1 November 2021

Bi, N., Yang, Z., Wang, H., Xu, C., & Guo, Z. (2014). Impact of artificial water and sediment discharge regulation in the Huanghe (Yellow River) on the transport of particulate heavy metals to the sea. *CATENA, 121*, 232–240. https://doi.org/10.1016/j.catena.2014.05.006

Biksham, G., & Subramanian, V. (1988). Sediment transport of the Godavari River basin and its controlling factors. *Journal of Hydrology, 101*, 275–290. https://doi.org/10.1016/0022-1694(88)90040-6

Blass, G., & Graf, H. W. (1995). Neufunde von Schlackenhalden in der nördlichen Eifel (II). *Mineralien Welt, 6*, 28–31.

Boenigk, W. (1978). *Die flußgeschichtliche Entwicklung der Niederrheinischen Bucht im Jungtertiär und Altquartär*. https://doi.org/10.23689/fidgeo-1651

Bogaart, P. W., van Balen, R. T., Vandenberghe, J., & Kasse, C. (2002). Process-based modelling of the climatic forcing of fluvial sediment flux: Some examples and a discussion of optimal model complexity. *Geological Society, London, Special Publications, 191*, 187–198. https://doi.org/10.1144/GSL.SP.2002.191.01.13

Brandt, S. (2000). Classification of geomorphological effects downstream of dams. *CATENA, 40*, 375–401. https://doi.org/10.1016/S0341-8162(00)00093-X

Brousse, G., Arnaud-Fassetta, G., Liébault, F., Bertrand, M., Melun, G., Loire, R., Malavoi, J.-R., Fantino, G., & Borgniet, L. (2020). Channel response to sediment replenishment in a large gravel-bed river: The case of the Saint-Sauveur dam in the Buëch River (Southern Alps, France). *River Research and Applications, 36*, 880–893. https://doi.org/10.1002/rra.3527

Bunte K (2004) State of the Science Review Gravel Mitigation and Augmentation Below Hydroelectric Dams: A Geomorphological Perspective

Callender, E. (2005). Heavy metals in the environment—historical trends. *Environmental Geochemistry, 9*, 67–105.

Chen, Z., Li, J., Shen, H., & Zhanghua, W. (2001). Yangtze River of China: Historical analysis of discharge variability and sediment flux. *Geomorphology, 41*, 77–91. https://doi.org/10.1016/S0169-555X(01)00106-4

Cheng, N.-S. (1997). Simplified settling velocity formula for sediment particle. *Journal of Hydraulic Engineering Division of the American Society of Civil Engineers, 123*, 149–152. https://doi.org/10.1061/(ASCE)0733-9429(1997)123:2(149)

Ciszewski, D., & Grygar, T. M. (2016). A review of flood-related storage and remobilization of heavy metal pollutants in river systems. *Water, Air, and Soil Pollution, 227*, 239. https://doi.org/10.1007/s11270-016-2934-8

Clark, D. E., Vogels, M. F. A., van der Perk, M., Owens, P. N., & Petticrew, E. L. (2014). Effects of a small-scale, abandoned gold mine on the geochemistry of fine stream-bed and floodplain sediments in the Horsefly River watershed, British Columbia, Canada. *Mineralogical Magazine, 78*, 1491–1504. https://doi.org/10.1180/minmag.2014.078.6.16

Cofalla, C. (2015). *Hydrotoxikologie—Entwicklung einer experimentellen Methodik zur Charakterisierung und Bewertung kohäsiver schadstoffbehafteter fluvialer Sedimente*. Dissertation, Universitätsbibliothek der RWTH Aachen

Collins, A. L., Walling, D. E., & Leeks, G. J. L. (1997). Sediment sources in the Upper Severn catchment: A fingerprinting approach. *Hydrology and Earth System Sciences, 1*, 509–521. https://doi.org/10.5194/hess-1-509-1997

Dai, Z., & Liu, J. T. (2013). Impacts of large dams on downstream fluvial sedimentation: An example of the Three Gorges Dam (TGD) on the Changjiang (Yangtze River). *Journal of Hydrology, 480*, 10–18. https://doi.org/10.1016/j.jhydrol.2012.12.003

Dhivert, E., Grosbois, C., Rodrigues, S., & Desmet, M. (2015). Influence of fluvial environments on sediment archiving processes and temporal pollutant dynamics (Upper Loire River, France). *Science of the Total Environment, 505*, 121–136. https://doi.org/10.1016/j.scitotenv.2014.09.082

DIN ISO 11277:2002–08, Bodenbeschaffenheit_- Bestimmung der Partikelgrößenverteilung in Mineralböden_- Verfahren mittels Siebung und Sedimentation (ISO_11277:1998_+ ISO_11277:1998 Corrigendum_1:2002), Berlin

East, A. E., Pess, G. R., Bountry, J. A., Magirl, C. S., Ritchie, A. C., Logan, J. B., Randle, T. J., Mastin, M. C., Minear, J. T., Duda, J. J., Liermann, M. C., McHenry, M. L., Beechie, T. J., & Shafroth, P. B. (2015). Large-scale dam removal on the Elwha River, Washington, USA: River channel and floodplain geomorphic change. *Geomorphology, 228*, 765–786. https://doi.org/10.1016/j.geomorph.2014.08.028

Elfers Geologische Schichten. http://www.wms.nrw.de/gd/GK100?VERSION=1.3.0&. Accessed 1 October 2021

Elsaeed, G.H., Aziz, M.S., Ziada, W.M. (2018). Sedimentation Future Prediction for Aswan High Dam Reservoir Using Mathematical Model Delft3D

Esser, V. (2020). *Untersuchungen zur fluvialen Morphodynamik und zur rezenten Schadstoffausbreitung in Flusssystemen—Beispiele aus der Grenzregion Belgien, Niederlande und Deutschland*. Dissertation, Rheinisch-Westfälische Technische Hochschule Aachen

Esser, V., Buchty-Lemke, M., Schulte, P., Podzun, L. S., & Lehmkuhl, F. (2020). Signatures of recent pollution profiles in comparable central European rivers—Examples from the international River Basin District Meuse. *CATENA, 193*, 104646. https://doi.org/10.1016/j.catena.2020.104646

European Environment Agency. (2016). *CLC 2018*. https://land.copernicus.eu/pan-european/corine-land-cover/clc2018. Accessed 19 October 2020

Eurostat. (2020). *Countries 2016: ref-countries-2016–01m.shp*. https://ec.europa.eu/eurostat/de/web/gisco/geodata/reference-data/administrative-units-statistical-units/countries. Accessed 20 October 2020

Fauth, H. (1985). *Geochemischer Atlas Bundesrepublik Deutschland: Verteilung von Schwermetallen in Wässern und Bachsedimenten*. Schweizerbart in Komm.

Ferguson, R. I. (1986). River loads underestimated by rating curves. *Water Resources Research, 22*, 74–76. https://doi.org/10.1029/WR022i001p00074

Foulds, S. A., Brewer, P. A., Macklin, M. G., Haresign, W., Betson, R. E., & Rassner, S. M. E. (2014). Flood-related contamination in catchments affected by historical metal mining: An unexpected and emerging hazard of climate change. *Science of the Total Environment, 476–477*, 165–180. https://doi.org/10.1016/j.scitotenv.2013.12.079

Franzius, O., Proetel, H. (1927). Der wasserwirtschaftliche Ausbau der Rur (Roer) in der Nord-Eifel. Denkschrift und vergleichende Entwürfe. Hamel'sche Druckerei, Düren

Frémion, F., Bordas, F., Mourier, B., Lenain, J.-F., Kestens, T., & Courtin-Nomade, A. (2016). Influence of dams on sediment continuity: A study case of a natural metallic contamination. *Science of the Total Environment, 547*, 282–294. https://doi.org/10.1016/j.scitotenv.2016.01.023

Gelfenbaum, G., Stevens, A. W., Miller, I., Warrick, J. A., Ogston, A. S., & Eidam, E. (2015). Large-scale dam removal on the Elwha River, Washington, USA: Coastal geomorphic change. *Geomorphology, 246*, 649–668. https://doi.org/10.1016/j.geomorph.2015.01.002

Geofabrik GmbH. (2018). gis_osm_waterways_free_1. CC BY-SA 2.0. download.geofabrik.de. Accessed 19 October 2020

Grams, P. E., Schmidt, J. C., & Topping, D. J. (2007). The rate and pattern of bed incision and bank adjustment on the Colorado River in Glen Canyon downstream from Glen Canyon Dam, 1956–2000. *Geological Society of America Bulletin, 119*, 556–575. https://doi.org/10.1130/B25969.1

Henkel S, Pummer E, Schüttrumpf H (2012) Wirtschaftliches Nutzungspotential deutscher Talsperrensedimente: Studie im Auftrag der Deutsche Rohstoffagentur (DERA) in der Bundesanstalt für Geowissenschaften und Rohstoffe (BGR)

Henkel, S., Pummer, E., Schüttrumpf, H., Schmitz, M., Schulz, S.-U. (2014). *Nutzungsmöglichkeiten und wirtschaftliches Potenzial deutscher Talsperrensedimente*, 2014th edn. DERA Rohstoffinformationen, vol 23. DERA, Berlin

Hillenbrand T, Toussaint D, Böhm E, Fuchs S, Scherer U, Rudolphi Aea (2005) Einträge von Kupfer, Zink und Blei in Gewässer und Böden. Analyse der Emissionspfade und möglicher Emissionsminderungsmaßnahmen;: Forschungsbericht 20224220/02

Hollert, H., Brinkmann, M., Hudjetz, S., Cofalla, C., & Schüttrumpf, H. (2014). Hochwasser - ein unterschätztes Risiko. *Biologie in Unserer Zeit, 44*, 44–51. https://doi.org/10.1002/biuz.201410527

Ibàñez, C., Prat, N., & Canicio, A. (1996). Changes in the hydrology and sediment transport produced by large dams on the lower Ebro river and its estuary. *Regulated Rivers: Research & Management, 12*, 51–62. https://doi.org/10.1002/(SICI)1099-1646(199601)12:1%3c51:AID-RRR376%3e3.0.CO;2-I

Intze, O. (1906). *Die geschichtliche Entwicklung, die Zwecke und der Bau der Talsperren*. Springer.

Issa, I. E., Al-Ansari, N., Knutsson, S., & Sherwany, G. (2015). Monitoring and evaluating the sedimentation process in Mosul dam reservoir using trap efficiency approaches. *ENG, 07*, 190–202. https://doi.org/10.4236/eng.2015.74015

Kabata-Pendias, A. (2011). *Trace elements in soils and plants* (4th ed.). CRC Press.

Kibler, K., Tullos, D., & Kondolf, M. (2011). Evolving Expectations of dam removal outcomes: Downstream geomorphic effects

following removal of a small, Gravel-Filled Dam1. *Journal of the American Water Resources Association, 47*, 408–423. https://doi.org/10.1111/j.1752-1688.2011.00523.x

Kondolf GM (1995) Managing bedload sediment in regulated rivers: Examples from California, U.S.A. In: Costa JE, Miller AJ, Potter KW, Wilcock PR (eds) *Natural and anthropogenic influences in fluvial geomorphology*, (vol. 89 pp. 165–176). American Geophysical Union, Washington, D. C.

Kondolf,. (1997). PROFILE: Hungry water: Effects of dams and gravel mining on river channels. *Environmental Management, 21*, 533–551. https://doi.org/10.1007/s002679900048

Krumbein, W. C., & Pettijohn, F. J. (1939). Manual of Sedimentary Petrography. XIV + 549 pp., 8:o, 265 fig. New York and London 1938, (1939). D. Appleton — Century Company. 8 6.50 (30 s.). *Geologiska Föreningen i Stockholm Förhandlingar, 61*, 225–227. https://doi.org/10.1080/11035893909452786

Legret, M., & Pagotto, C. (1999). Evaluation of pollutant loadings in the runoff waters from a major rural highway. *Science of the Total Environment, 235*, 143–150. https://doi.org/10.1016/S0048-9697(99)00207-7

Lehmkuhl F (2011) Die Entstehung des heutigen Naturraums und seine Nutzung. In: Kraus T, Pohle F (eds) *Die natürlichen Grundlagen - von der Vorgeschichte bis zu den Karolingern*, pp. 87–129

Luo, X. X., Yang, S. L., & Zhang, J. (2012). The impact of the Three Gorges Dam on the downstream distribution and texture of sediments along the middle and lower Yangtze River (Changjiang) and its estuary, and subsequent sediment dispersal in the East China Sea. *Geomorphology, 179*, 126–140. https://doi.org/10.1016/j.geomorph.2012.05.034

Maaß, A.-L., & Schüttrumpf, H. (2018). Long-term effects of mining-induced subsidence on the trapping efficiency of floodplains. *Anthropocene, 24*, 1–13. https://doi.org/10.1016/j.ancene.2018.10.001

Maaß, A.-L., & Schüttrumpf, H. (2019a). Elevated floodplains and net channel incision as a result of the construction and removal of water mills. *Geografiska Annaler: Series a, Physical Geography, 101*, 157–176. https://doi.org/10.1080/04353676.2019.1574209

Maaß, A.-L., & Schüttrumpf, H. (2019b). Reactivation of floodplains in river restorations: Long-term implications on the mobility of floodplain sediment deposits. *Water Resources Research, 10*, 1. https://doi.org/10.1029/2019WR024983

Maaß, A.-L., Schüttrumpf, H., & Lehmkuhl, F. (2021). Human impact on fluvial systems in Europe with special regard to today's river restorations. *Environmental Sciences Europe*. https://doi.org/10.1186/s12302-021-00561-4

MacDonald, D. D., Ingersoll, C. G., & Berger, T. A. (2000). Development and evaluation of consensus-based sediment quality guidelines for freshwater ecosystems. *Archives of Environmental Contamination and Toxicology, 39*, 20–31. https://doi.org/10.1007/s002440010075

Major, J., O'Connor, J., Podolak, C. J., Keith, M. K., Grant, G. E., Spicer, K. R., Pittman, S., Bragg, H. M., Wallick, J. R., Tanner, D. Q., Rhode, A., Wilcock, P. R. (2012). Geomorphic response of the Sandy River, Oregon, to removal of Marmot Dam. Professional Paper 1792. https://pubs.usgs.gov/pp/1792/pp1792_text.pdf. Accessed 12 Dec 2021

Marcinkowski, P., & Grygoruk, M. (2017). Long-term downstream effects of a dam on a lowland river flow regime: Case study of the upper Narew. *Water, 9*, 783. https://doi.org/10.3390/w9100783

McBean, E. A., & Al-Nassri, S. (1988). Uncertainty in suspended sediment transport curves. *Journal of Hydraulic Engineering Division of the American Society of Civil Engineers, 114*, 63–74. https://doi.org/10.1061/%28ASCE%290733-9429%281988%29114%3A1%2863%29

Meybeck, M., Lestel, L., Bonté, P., Moilleron, R., Colin, J. L., Rousselot, O., Hervé, D., de Pontevès, C., Grosbois, C., & Thévenot, D. R. (2007). Historical perspective of heavy metals contamination (Cd, Cr, Cu, Hg, Pb, Zn) in the Seine River basin (France) following a DPSIR approach (1950–2005). *Science of the Total Environment, 375*, 204–231. https://doi.org/10.1016/j.scitotenv.2006.12.017

Miller, J., Barr, R., Grow, D., Lechler, P., Richardson, D., Waltman, K., & Warwick, J. (1999). Effects of the 1997 flood on the transport and storage of sediment and mercury within the Carson River Valley, West-Central Nevada. *The Journal of Geology, 107*, 313–327. https://doi.org/10.1086/314353

Milliman, J. D., & Syvitski, J. P. M. (1992). Geomorphic/tectonic control of sediment discharge to the ocean: The importance of small mountainous rivers. *The Journal of Geology, 100*, 525–544. https://doi.org/10.1086/629606

Ministerium für Umwelt, Landwirtschaft, Natur- und Verbraucherschutz NRW. (2021). ELWAS-WEB: Karte. www.elwasweb.nrw.de. Accessed 24 November 2021

MKULNV NRW. (2015). *Steckbriefe der Planungseinheiten in den nordrhein-westfälischen Anteilen von Rhein, Weser, Ems und Maas: Bewirtschaftungsplan 2016–202*. https://docplayer.org/79864940-Steckbriefe-der-planungseinheiten-in-den-nordrhein-westfaelischen-anteilen-von-rhein-weser-ems-und-maas-bewirtschaftungsplan.html. Accessed 10 February 2022

Monaci, F., & Bargagli, R. (1997). Barium and other trace metals as indicators of vehicle emissions. *Water, Air, and Soil Pollution, 100*, 89–98. https://doi.org/10.1023/A:1018318427017

Mool, P., Popescu, I., Giri, S., Omer, A., Sloff, K., Kitamura, Y., Solomatine, D. (2017). Delft3D morphological modelling of sediment management in daily peaking run-of-the-river hydropower (PROR) reservoirs in Nepal. In: *Proc., 85th Annual Meeting of Int. Commission on Large Dams*. Paris: International Commission on Large Dams

Morgan, J. A., & Nelson, P. A. (2019). Morphodynamic modeling of sediment pulse dynamics. *Water Resources Research, 55*, 8691–8707. https://doi.org/10.1029/2019WR025407

Nelson, N. C., Erwin, S. O., & Schmidt, J. C. (2013). Spatial and temporal patterns in channel change on the Snake River downstream from Jackson Lake dam, Wyoming. *Geomorphology, 200*, 132–142. https://doi.org/10.1016/j.geomorph.2013.03.019

Nilson, E., Lehmkuhl, F. (2006). *Landschaftstransformation am Eifelnordrand seit Beginn der industriellen Revolution: Räumliche Auswirkungen geogener Faktoren*. Natur am Niederrhein :47–60

Nilson, E. (2006b). *Räumlich-strukturelle und zeitlich-dynamische Aspekte des Landnutzungswandels im Dreiländereck Belgien-Niederlande-Deutschland: Eine Analyse mittels eines multitemporalen, multifaktoriellen und grenzübergreifenden Geographischen Informationssystems*. Aachen, Techn. Hochsch., Diss., 2006b

Nilson, E. (2006a). Flusslandschaften im Wandel: Untersuchungen zur Mäanderentwicklung an zwei Maas-Tributären anhand von historischem Bild-und Kartenmaterial. *Grenzüberschreitendes Integratives Gewässermanagement, 1*, 111–125.

Nilsson, C., Reidy, C. A., Dynesius, M., & Revenga, C. (2005). Fragmentation and flow regulation of the world's large river systems. *Science, 308*, 405–408. https://doi.org/10.1126/science.1107887

Pal, S. (2016). Impact of Massanjore Dam on hydro-geomorphological modification of Mayurakshi River, Eastern India. *Environment, Development and Sustainability, 18*, 921–944. https://doi.org/10.1007/s10668-015-9679-1

Palanques, A., Grimalt, J., Belzunces, M., Estrada, F., Puig, P., & Guillén, J. (2014). Massive accumulation of highly polluted sedimentary deposits by river damming. *Science of the Total Environment, 497–498*, 369–381. https://doi.org/10.1016/j.scitotenv.2014.07.091

Panagos, P., Ballabio, C., Poesen, J., Lugato, E., Scarpa, S., Montanarella, L., & Borrelli, P. (2020). A soil erosion indicator for supporting agricultural, environmental and climate policies in the European Union. *Remote Sensing, 12*, 1365. https://doi.org/10.3390/rs12091365

Paul J (1994) Grenzen der Belastbarkeit: Die Flüsse Rur (Roer) und Inde im Industriezeitalter. Forum Jülicher Geschichte, vol 10. Joseph-Kuhl-Gesellschaft zur Geschichte der Stadt Jülich und des Jülicher Landes, Jülich

Paul, J. (1999). Vom reißenden Gewässer zum gebändigten Fluß.: Die Geschichte der Wasserwirtschaft im Flußgebiet der Rur vom 16. Jahrundert bis in die Zeit um 1960. In: Wasserverband Eifel-Rur (ed) *100 Jahre Wasserwirtschaft in der Nordeifel*, Düren, pp. 51–62.

Petts, G. E. (1979). Complex response of river channel morphology subsequent to reservoir construction. *Progress in Physical Geography: Earth and Environment, 3*, 329–362. https://doi.org/10.1177/030913337900300302

Phillips, J. D., Slattery, M. C., & Musselman, Z. A. (2005). Channel adjustments of the lower Trinity River, Texas, downstream of Livingston Dam. *Earth Surface Processes and Landforms, 30*, 1419–1439. https://doi.org/10.1002/esp.1203

Polczyk, H. (1999b), Die Talsperren der Nordeifel. In: *100 Jahre Wasserwirtschaft in der Nordeifel*, pp. 64–72.

Polczyk, H. (1999a). *Bewirtschaftung eines Talsperrenverbundsystems mit verschiedenen Nutzungen. Betrieb, Instandsetzung und Modernisierung von Wasserbauwerken*. Dresdner Wasserbauliche Mitteilungen, pp. 89–102.

Pye, K., & Blott, S. J. (2004). Particle size analysis of sediments, soils and related particulate materials for forensic purposes using laser granulometry. *Forensic Science International, 144*, 19–27. https://doi.org/10.1016/j.forsciint.2004.02.028

Rahmani, V., Kastens, J., deNoyelles, F., Jakubauskas, M., Martinko, E., Huggins, D., Gnau, C., Liechti, P., Campbell, S., Callihan, R., & Blackwood, A. (2018). Examining storage capacity loss and sedimentation rate of large reservoirs in the central U.S. Great Plains. *Water, 10*, 190. https://doi.org/10.3390/w10020190

Reichert, J. (2021). *Hochwasserkatastrophe im Juli 2021 - Einordnung, Ablauf und Konsequenzen -: Presentation*. Mitgliederversammlung der AG Wasserkraftwerke NRW, Düren

Resongles, E., Casiot, C., Freydier, R., Dezileau, L., Viers, J., & Elbaz-Poulichet, F. (2014). Persisting impact of historical mining activity to metal (Pb, Zn, Cd, Tl, Hg) and metalloid (As, Sb) enrichment in sediments of the Gardon River, Southern France. *Science of the Total Environment, 481*, 509–521. https://doi.org/10.1016/j.scitotenv.2014.02.078

Rollet, A. J., Piégay, H., Dufour, S., Bornette, G., & Persat, H. (2014). Assessment of consequences of sediment deficit on a gravel river bed downstream of dams in restoration perspectives: Application of a multicriteria, hierarchical and spatially explicit diagnosis. *River Research and Applications, 30*, 939–953. https://doi.org/10.1002/rra.2689

Rovira, A., & Ibàñez, C. (2007). Sediment management options for the lower Ebro River and its delta. *Journal of Soils and Sediments, 7*, 285–295. https://doi.org/10.1065/jss2007.08.244

Saam, L., Mouris, K., Wieprecht, S., Haun, S. (2019). Three-dimensional numerical modelling of reservoir flushing to obtain long-term sediment equilibrium. In: *38th IAHR World Congress - "Water: Connecting the World". The International Association for Hydro-Environment Engineering and Research* (IAHR), pp. 2364–2371.

Salomons, W., & Förstner, U. (1984). *Metals in the Hydrocycle*. Springer.

Sanyal, J., Lauer, J. W., & Kanae, S. (2021). Examining the downstream geomorphic impact of a large dam under climate change. *CATENA*. https://doi.org/10.1016/j.catena.2020.104850

Scheuch, H. (1967). *Wasserwirtschaflicher Rahmenplan Rur*. (Eifelrur). Landesvermessungsamt Nordrhein-Westfalen, Düsseldorf

Schintu, M., Kudo, A., Sarritzu, G., & Contu, A. (1991). Heavy metal distribution and mobilization in sediments from a drinking water reservoir near a mining area. *Water, Air, and Soil Pollution, 57–58*, 329–338. https://doi.org/10.1007/bf00282896

Schmidt, J. C., & Wilcock, P. R. (2008). Metrics for assessing the downstream effects of dams. *Water Resources Research*. https://doi.org/10.1029/2006WR005092

Schulte, P., Lehmkuhl, F., Steininger, F., Loibl, D., Lockot, G., Protze, J., Fischer, P., & Stauch, G. (2016). Influence of HCl pretreatment and organo-mineral complexes on laser diffraction measurement of loess–paleosol-sequences. *CATENA, 137*, 392–405. https://doi.org/10.1016/j.catena.2015.10.015

Sojka, M., Jaskuła, J., & Siepak, M. (2019). Heavy Metals in bottom sediments of reservoirs in the lowland area of western Poland: Concentrations, distribution, Sources and Ecological Risk. *Water, 11*, 56. https://doi.org/10.3390/w11010056

SPECTRO. (2007). *Analysis of Trace Elements in Geological Materials*. Soils and Sludges Prepared as Pressed Pellets.

Stauch, G., Esch, A., Dörwald, L., Esser, V., Lechthaler, S., Lehmkuhl, F., Schulte, P., Walk, J. (2021). *115 years of sediment deposition in the Urft reservoir (Eifel Mountains, western Germany)*. EGU General Assembly 2021 19–30 Apr 2021:EGU21-148. https://doi.org/10.5194/egusphere-egu21-148

Sutherland, A. J. (1987). Static armour layers by selective erosion. In C. R. Thorne (Ed.), *Sediment transport in gravel-bed rivers.* Wiley.

Szarek-Gwiazda, E., Czaplicka-Kotas, A., & Szalińska, E. (2011). Background concentrations of nickel in the sediments of the Carpathian dam reservoirs (Southern Poland). *Clean: Soil, Air, Water, 39*, 368–375. https://doi.org/10.1002/clen.201000114

Szatten, D., & Habel, M. (2020). Effects of land cover changes on sediment and nutrient balance in the catchment with cascade-dammed waters. *Remote Sensing, 12*, 3414. https://doi.org/10.3390/rs12203414

Turner, R. E., Qureshi, N., Rabalais, N. N., Dortch, Q., Justić, D., Shaw, R. F., & Cope, J. (1998). Fluctuating silicate:Nitrate ratios and coastal plankton food webs. *Proceedings of the National Academy of Sciences of the United States of America, 95*, 13048–13051. https://doi.org/10.1073/pnas.95.22.13048

UMWELTBUNDESAMT (2001) *Abtrag von Kupfer und Zink von Dächern, Dachrinnen und Fallrohren durch Niederschläge*. https://www.umweltbundesamt.de/sites/default/files/medien/publikation/long/3587.pdf. Accessed 17 December 2021

van Maren, D. S., Yang, S.-L., & He, Q. (2013). The impact of silt trapping in large reservoirs on downstream morphology: The Yangtze River. *Ocean Dynamics, 63*, 691–707. https://doi.org/10.1007/s10236-013-0622-4

Walling DE (1977) Limitations of the rating curve technique for estimating suspended sediment loads, with particular reference to British rivers. In: *Erosion and solid matter transport in inland waters*, (vol 122, pp. 34–48). IAHS Publication

Walling DE (2012) *The role of dams in the global sediment budget. Erosion and Sediment Yields in the Changing Environment* (Proceedings of a symposium held at the Institute of Mountain Hazards and Environment, CAS-Chengdu, China, 11–15 October 2012). IAHS Publ. :3–11

Walling, D., Owens, P., Carter, J., Leeks, G., Lewis, S., Meharg, A., & Wright, J. (2003). Storage of sediment-associated nutrients and contaminants in river channel and floodplain systems. *Applied Geochemistry, 18*, 195–220. https://doi.org/10.1016/S0883-2927(02)00121-X

Wasserverband Eifel-Rur (ed) (1999) 100 Jahre Wasserwirtschaft in der Nordeifel, Düren

Wasserverband Eifel-Rur (2017a) Die Rurtalsperre. https://wver.de/wp-content/uploads/2019/11/Rurtalsperre.pdf. Accessed 24 November 2021

Wasserverband Eifel-Rur (2017b) Die Stauanlage Heimbach. https://wver.de/wp-content/uploads/2019/11/stb_heimbach.pdf. Accessed 2 December 2021

Wasserverband Eifel-Rur (2017c) Die Stauanlage Obermaubach. https://wver.de/wp-content/uploads/2019/11/stb_obermaubach.pdf. Accessed 2 December 2021

Wasserverband Eifel-Rur (2021) Faktencheck zum Hochwasser. https://wver.de/faktencheck-zum-hochwasser/. Accessed 23 September 2021

Weiss, S. (1990a). *Atlas der Mineralfundstellen in Deutschland-West: Beschreibung von 1038 Fundstellen im Gebiet von Deutschland-West; mit 56 farbigen Kartenausschnitten im Maßstab 1:300.000 mit Fundstellen-Eintragungen*. Weise.

Weiss, S. (1990b). *Atlas der Mineralfundstellen in Deutschland-West: Beschreibung von 1038 Fundstellen im Gebiet von Deutschland-West; mit 56 farbigen Kartenausschnitten im Maßstab 1:300.000 mit Fundstellen-Eintragungen*. Weise.

Weller, H. (1988). Milieuinterpretation von Korngrößen-Summenkurven am Beispiel verfestigter Molasse-Sandsteine. *Zeitschrift Für Geologische Wissenschaften, 16*, 299–309.

Westerhoff, W. E., Kemna, H. A., & Boenigk, W. (2008). The confluence area of Rhine, Meuse, and Belgian rivers: Late Pliocene and Early Pleistocene fluvial history of the northern Lower Rhine Embayment. *Netherlands Journal of Geosciences, 87*, 107–125. https://doi.org/10.1017/S0016774600024070

Williams, G. P., Wolman, M. G. (1984). Downstream effects of dams on alluvial rivers. GEOLOGICAL SURVEY PROFESSIONAL PAPER

Wisser, D., Frolking, S., Hagen, S., & Bierkens, M. F. P. (2013). Beyond peak reservoir storage? A global estimate of declining water storage capacity in large reservoirs. *Water Resources Research, 49*, 5732–5739. https://doi.org/10.1002/wrcr.20452

Wolf, S., Esser, V., Schüttrumpf, H., & Lehmkuhl, F. (2021). Influence of 200 years of water resource management on a typical central European river. Does industrialization straighten a river? *Environmental Sciences Europe*. https://doi.org/10.1186/s12302-021-00460-8

Yang, S. L., Milliman, J. D., Xu, K. H., Deng, B., Zhang, X. Y., & Luo, X. X. (2014). Downstream sedimentary and geomorphic impacts of the Three Gorges Dam on the Yangtze River. *Earth-Science Reviews, 138*, 469–486. https://doi.org/10.1016/j.earscirev.2014.07.006

Yang, S. L., Zhang, J., & Xu, X. J. (2007). Influence of the Three Gorges Dam on downstream delivery of sediment and its environmental implications, Yangtze River. *Geophysical Research Letters*. https://doi.org/10.1029/2007GL029472

Zhao, Q., Liu, S., Deng, L., Dong, S., & Wang, C. (2013). Longitudinal distribution of heavy metals in sediments of a canyon reservoir in Southwest China due to dam construction. *Environmental Monitoring and Assessment, 185*, 6101–6110. https://doi.org/10.1007/s10661-012-3010-5

Ziegler, C. K., & Nisbet, B. S. (1995). Long-term simulation of fine-grained sediment transport in large reservoir. *Journal of Hydraulic Engineering Division of the American Society of Civil Engineers, 121*, 773–781. https://doi.org/10.1061/(ASCE)0733-9429(1995)121:11(773)

Ziliani, L., & Surian, N. (2012). Evolutionary trajectory of channel morphology and controlling factors in a large gravel-bed river. *Geomorphology, 173–174*, 104–117. https://doi.org/10.1016/j.geomorph.2012.06.001